



Research article

$\bar{\partial}$ -dressing method for the three-coupled fourth-order nonlinear Schrödinger system

Jin-Jin Mao*and Xue-Wei Yan

College of Science, Nanjing University of Posts and Telecommunications, Nanjing, 210023, China

* **Correspondence:** Email: mao_jinjin0806@163.com, jj-mao@njupt.edu.cn.

Abstract: This article mainly investigated the three-coupled fourth-order nonlinear Schrödinger (NLS) systems, which characterized the alpha-helical proteins with interspine coupling at the fourth-order interaction. By the $\bar{\partial}$ -dressing method, we studied the three-coupled fourth-order NLS systems. We derived a new spectral problem starting from the $\bar{\partial}$ -problem. Then, we obtained the three-coupled fourth-order NLS hierarchy associated with the spectral problem using a recursive operator. Finally, we analyzed the N -soliton solutions of the three-coupled fourth-order NLS systems by determining the spectral transform matrix in the $\bar{\partial}$ -problem. We also provided detailed descriptions of the 1-, 2-, and 3-soliton solutions, along with dynamic features and graphical illustration.

Keywords: the three-coupled fourth-order nonlinear Schrödinger systems; $\bar{\partial}$ -dressing method; Lax pair; recursive operator; soliton solutions

Mathematics Subject Classification: 30E25, 35Q15

1. Introduction

The nonlinear Schrödinger (NLS) equation contributes greatly to various fields of nonlinear science, such as nonlinear optics [1–3], plasma physics [4], biological physics [5], hydrodynamics [6], even finance [7], and atmosphere situations [8]. Over recent decades, a variety of analytical methods have been developed to study such nonlinear systems. Among these, the Darboux transformation provides an algebraic iterative procedure for constructing soliton solutions and has been widely applied to integrable systems such as the NLS family [9, 10], the Sasa-Satsuma equation [11], and the coupled Fokas-Lenells system [12]. The Hirota bilinear method offers a direct approach for deriving explicit multi-soliton solutions via a clever variable transformation and remains fundamental to soliton theory [13, 14]. For solving initial-value problems, the inverse scattering transform serves as a cornerstone technique, offering a nonlinear analog to the Fourier transform and a complete integrability framework for key equations including the Korteweg-de Vries (KdV) equation [15, 16], and the NLS

equations [17, 18].

In addition to their fundamental mathematical interest, solitons described by the NLS-type equations have found a broad range of physical and technological applications in recent years. For example, the collapse of soliton-like bubbles induced by cavitation has been exploited to launch microbots in biomedical systems [19]. Optical solitons have also been experimentally realized in photonic Moir lattices [20]. Moreover, soliton dynamics plays a central role in modern optical communication and photonics, where solitons are employed for coded signal transmission [21] and as stable pulse structures in fiber lasers [22]. These advances highlight the practical importance of solitons and further motivate the theoretical exploration of multi-component and higher-order integrable systems capable of modeling such nonlinear wave phenomena.

In recent years, the study about generalized NLS equations has garnered significant attention. For example, Scott [23] first explored the application of coupled NLS equations to alpha-helical proteins. Veni and Latha [24] proposed generalized model to describe the dynamics of alpha-helical proteins incorporating inter-spike coupling. This model incorporates excitations of both quadrupole and dipole types, next-nearest-neighbor and nearest-neighbor interactions, as well as higher-order interspine couplings. In this article, we focus on the investigation of the following three-coupled fourth-order NLS systems [24]

$$\begin{aligned} iq_{j,t} + q_{j,xx} + 2 \sum_{\rho=1}^3 |q_{\rho}|^2 q_j + \gamma \left[q_{j,xxxx} + 2 \sum_{\rho=1}^3 |q_{\rho,x}|^2 q_j + 2 \sum_{\rho=1}^3 q_{\rho} \bar{q}_{\rho,x} q_{j,x} + 6 \sum_{\rho=1}^3 \bar{q}_{\rho} q_{\rho,x} q_{j,x} \right. \\ \left. + 4 \sum_{\rho=1}^3 |q_{\rho}|^2 q_{j,xx} + 4 \sum_{\rho=1}^3 \bar{q}_{\rho} q_{\rho,xx} q_j + 2 \sum_{\rho=1}^3 q_{\rho} \bar{q}_{\rho,xx} q_j + 6 \left(\sum_{\rho=1}^3 |q_{\rho}|^2 \right)^2 q_j \right] = 0, \quad (j = 1, 2, 3), \end{aligned} \quad (1.1)$$

where q_j represents the wave envelopes, γ is the lattice parameter, \bar{q} represents the complex conjugate of q , and x and t correspond to the scaled distance and delay time, respectively. Recently, various methods have been employed to study the three-coupled fourth-order NLS systems given by (1.1). For instance, Veni and Latha obtained the multi-soliton solutions of the three-coupled fourth-order NLS systems (1.1) using the Darboux transformation in Ref. [24]; Sun, Tian, Wang, and Zhen derived the bilinear forms and multi-soliton solutions of the equations (1.1) using the binary Bell-polynomial approach [25]; Du, Tian, and colleagues investigated semirational rogue waves, rational and semirational rogue waves, and vector multi-rogue wave solutions of the three-coupled fourth-order NLS systems (1.1) via the generalized Darboux transformation in 2017 [5, 26, 27]; Dong, Tian, and Wei obtained infinitely many conservation laws and constructed some semirational solutions of the equations (1.1) using the Darboux-dressing transformations [28].

Moreover, it is well known that when $\gamma = 0$, the three-coupled fourth-order NLS systems (1.1) reduce to the three-component coupled NLS equation. Zhao and Liu obtained its vector rogue waves using the Darboux transformation [29], while Wang and Han studied its breather waves and rogue waves using the Darboux-dressing transformations [30]. When $\gamma = 0$ and $j = 1, 2$, the three-coupled fourth-order NLS systems (1.1) reduce to the dimensionless vector NLS equation, and Baronio et al. investigated its semi-rational, multi-parametric vector solutions [31]. Although significant progress has been made in constructing soliton solutions for the three-component fourth-order NLS system (1.1), to the best of our knowledge, relatively few studies have addressed the derivation of the full integrable hierarchy associated with such systems. In this article, we employ the $\bar{\partial}$ -problem framework to derive

the three-component fourth-order NLS hierarchy and to investigate the soliton dynamical behaviors arising in this context.

Although methods such as Darboux and Bäcklund transformations have proven highly effective for generating soliton solutions in integrable systems, they often rely on specific ansätze and typically require iterative procedures to construct multi-soliton configurations. Similarly, binary Bell polynomials and the Hirota bilinear method are effective tools when applied to systems admitting a bilinear form. However, their applicability becomes limited in the presence of higher-order couplings or non-standard Lax structures. In contrast, the $\bar{\partial}$ -dressing method offers significant advantages in solving nonlocal spectral problems. Notably, this approach does not depend on the existence of a bilinear form, making it well suited (for more general integrable systems) particularly those involving higher-order derivatives and strongly coupled multi-component structures. Moreover, the $\bar{\partial}$ -dressing method facilitates the construction of the entire integrable hierarchy within a unified spectral framework, rather than being restricted to isolated solutions. This model not only broadens the scope of analytical techniques but also provides an influential tool for systematically uncovering the underlying algebraic and geometric structures of the model, thereby offering a deeper understanding of its integrability.

The $\bar{\partial}$ -dressing method, an effective analytical tool for constructing soliton solutions of nonlinear integrable systems, was first introduced by Zakharov and Shabat in 1974 [32]. Since then, it has been extensively applied to study various properties of nonlinear equations, including their long-time asymptotic behavior, transformation structures, and reduction processes [33, 34]. The method remains active in contemporary research, being employed to derive integrable hierarchies and explicit solutions for a wide range of systems [35, 36], such as the Kadomtsev-Petviashvili (KP) I equation [37], the Ablowitz-Barseghyan (AB) equations [38], the Davey-Stewartson II (DS-II) equation [39], the three-wave interaction system [40], the Kaup-Broer system [41], the coupled Gerdjikov-Ivanov equation [42], the nonlocal extended modified KdV equation [43], and the differential-difference KP equation [44, 45].

However, to the best of our knowledge, the application of the $\bar{\partial}$ -dressing method to coupled multi-component systems (particularly those of higher order) has not been explored in the existing research. Motivated by this gap, the present work focuses on extending the $\bar{\partial}$ -dressing framework to analyze the three-coupled fourth-order NLS systems. Specifically, we construct the associated spectral transform matrix for the $\bar{\partial}$ -problem, derive the corresponding integrable hierarchy, and obtain the explicit N -soliton solutions. In addition, visualize and investigate the nature of soliton interactions within this system, we present both three-dimensional plots and characteristic line diagrams of 1-, 2-, and 3-soliton solutions.

The structure of this article is organized as follows: In Sect. 2, we introduce the $\bar{\partial}$ -problem and construct the spatial and time spectral problems using the $\bar{\partial}$ -problem method. In Sect. 3, we derive the three-coupled fourth-order NLS hierarchy using recursive operators. In Sect. 4, we derive the N -soliton solutions of the three-coupled fourth-order NLS systems (1.1), based on the spectral transform matrix derived from the $\bar{\partial}$ -problem introduced in Sect. 2. Additionally, we present the 1-, 2- and 3-soliton solutions, together with their graphical representations, to more effectively illustrate the underlying dynamical phenomena.

2. Spectral problems and Lax pair

2.1. The spatial spectral problem

We consider the special $\bar{\partial}$ -problem

$$\bar{\partial}\Psi(x, t, \lambda) = \Psi(x, t, \lambda)R(x, t, \lambda), \quad (2.1)$$

where $\Psi(x, t, \lambda)$ and $R(x, t, \lambda)$ are 4×4 matrices, $\lambda \in \mathbb{C}$ denotes the complex spectral parameter, and $\bar{\partial}$ denotes the complex derivative with respect to the conjugate variable $\bar{\lambda}$ (i.e. $\bar{\partial} = \frac{\partial}{\bar{\lambda}}$). We suppose that

$$\Psi(x, t, \lambda) \rightarrow \mathbb{I}, \text{ as } \lambda \rightarrow \infty,$$

where \mathbb{I} means a 4×4 identity matrix. Then, the $\bar{\partial}$ -problem (2.1) satisfies the following solution

$$\Psi(x, t, \lambda) = \mathbb{I} + \frac{1}{2\pi i} \int \int \frac{\Psi(\xi)R(\xi)}{\xi - \lambda} d\xi \wedge d\bar{\xi} = \mathbb{I} + \Psi R C_\lambda, \quad (2.2)$$

where C_λ means the left Cauchy-Green integral operator and $\bar{\xi}$ represents the complex conjugate of ξ . From Eq (2.2), we get the formal solution of the $\bar{\partial}$ -problem (2.1)

$$\Psi(\lambda) = (\mathbb{I} - RC_\lambda)^{-1}, \quad (2.3)$$

where the superscript -1 denotes the inverse of the matrix. To simplify our presentation, we define two pairings

$$\langle f, g \rangle = \frac{1}{2\pi i} \int \int f(\lambda)g^\top(\lambda) d\lambda \wedge d\bar{\lambda}, \quad \langle f \rangle = \langle f, \mathbb{I} \rangle = \frac{1}{2\pi i} \int \int f(\lambda) d\lambda \wedge d\bar{\lambda},$$

where the superscript \top denotes the transpose of a matrix, which satisfies the following three properties

$$\langle f, g \rangle^\top = \langle g, f \rangle, \quad \langle fR, g \rangle = \langle f, gR^\top \rangle, \quad \langle fC_\lambda, g \rangle = -\langle f, gC_\lambda \rangle. \quad (2.4)$$

For matrix functions $f(\lambda)$ and $g(\lambda)$, our calculation shows that

$$g(\lambda)[f(\lambda)C_\lambda]C_\lambda + [g(\lambda)C_\lambda]f(\lambda)C_\lambda = [g(\lambda)C_\lambda][f(\lambda)C_\lambda].$$

The Lax pair of nonlinear equations is fundamental to various methods, such as the Darboux transformation, algebraic geometry method, Riemann-Hilbert method, inverse scattering transform, and others. If the transformation matrix $R(x, t, \lambda)$ satisfies a simple linear equation, then the Lax pair of the three-coupled fourth-order NLS systems (1.1) can be constructed from the $\bar{\partial}$ -problem (2.1).

Proposition 1 *Let the transform matrix $R(x, t, \lambda)$ satisfy the following form*

$$R_x = -i\lambda[R, \sigma], \quad (2.5)$$

where $\sigma = \text{diag}(1, -1, -1, -1)$, then the solution Ψ of the $\bar{\partial}$ -problem (2.1) satisfies the spatial spectral problem of the three-coupled fourth-order NLS systems (1.1) as

$$\Psi_x - i\lambda[\sigma, \Psi] = P\Psi, \quad (2.6)$$

with

$$P = \begin{pmatrix} 0 & \bar{q}_1 & \bar{q}_2 & \bar{q}_3 \\ -q_1 & 0 & 0 & 0 \\ -q_2 & 0 & 0 & 0 \\ -q_3 & 0 & 0 & 0 \end{pmatrix} = i[\sigma, \langle \Psi R \rangle]. \quad (2.7)$$

Proof Through Eqs (2.3) and (2.5), we have

$$\Psi_x = -i\lambda\Psi R\sigma C_\lambda(\mathbb{I} - RC_\lambda)^{-1} + i\lambda\Psi\sigma RC_\lambda(\mathbb{I} - RC_\lambda)^{-1}. \quad (2.8)$$

Direct calculation shows that

$$\begin{aligned} \lambda\Psi RC_\lambda &= \langle \Psi R \rangle + \lambda(\Psi - \mathbb{I}), \\ \lambda^2\Psi RC_\lambda &= \langle \lambda\Psi R \rangle + \lambda\langle \Psi R \rangle + \lambda^2(\Psi - \mathbb{I}), \\ \lambda^3\Psi RC_\lambda &= \langle \lambda^2\Psi R \rangle + \lambda\langle \lambda\Psi R \rangle + \lambda^2\langle \Psi R \rangle + \lambda^3(\Psi - \mathbb{I}), \\ \lambda^4\Psi RC_\lambda &= \langle \lambda^3\Psi R \rangle + \lambda\langle \lambda^2\Psi R \rangle + \lambda^2\langle \lambda\Psi R \rangle + \lambda^3\langle \Psi R \rangle + \lambda^4(\Psi - \mathbb{I}). \end{aligned} \quad (2.9)$$

On the basis of $RC_\lambda = \mathbb{I} - (\mathbb{I} - RC_\lambda)$, we get

$$RC_\lambda(\mathbb{I} - RC_\lambda)^{-1} = (\mathbb{I} - RC_\lambda)^{-1} - \mathbb{I}. \quad (2.10)$$

Substituting the first formula of Eqs (2.9) and Eq (2.10) into Eq (2.8), we have

$$\Psi_x = -i\langle \Psi R \rangle\sigma\Psi + i\lambda\sigma(\mathbb{I} - RC_\lambda)^{-1} - i\lambda\Psi\sigma. \quad (2.11)$$

From the first formula of Eq (2.9), it can be found that

$$\lambda(\mathbb{I} - RC_\lambda)^{-1} = \langle \Psi R \rangle\Psi + \lambda\Psi. \quad (2.12)$$

Substituting Eq (2.12) into Eq (2.11), we obtain

$$\Psi_x - i\lambda[\sigma, \Psi] = i[\sigma, \langle \Psi R \rangle]\Psi.$$

By taking $P = i[\sigma, \langle \Psi R \rangle]$, the proof is finished.

2.2. The time spectral problem

Proposition 2 Let the transform matrix $R(x, t, \lambda)$ satisfy the following form

$$R_t = [R, \Omega], \quad (2.13)$$

where Ω indicates the dispersion relation depending on x and t . We decompose Ω into the polynomial part Ω_p and the singularity part Ω_s , namely,

$$\Omega = \Omega_p + \Omega_s = \alpha_n\lambda^n\sigma + \frac{1}{2\pi i} \int \int \frac{\omega(\xi)\sigma}{\xi - \lambda} d\xi \wedge d\bar{\xi}, \quad (2.14)$$

where α_n represents constant and $\bar{\partial}\Omega_s = \omega(\lambda)\sigma$. Then, the solution Ψ of the $\bar{\partial}$ -problem (2.1) satisfies time spectral problem of the three-coupled fourth-order NLS systems (1.1) as

$$\Psi_t + (8i\gamma\lambda^4 - 2i\lambda^2)[\sigma, \Psi] = -8\gamma\lambda^3P\Psi + 4i\gamma\lambda^2\sigma(P_x - P^2)\Psi + 2\gamma\lambda(P_{xx} + PP_x - P_xP - 2P^3)\Psi$$

$$+ 2\lambda P\Psi + i\gamma\sigma(-P_{xxx} + PP_{xx} + P_{xx}P - 3P^4 - P_x^2 + 3P^2P_x + 3P_xP^2)\Psi + i\sigma(P^2 - P_x)\Psi. \quad (2.15)$$

Proof We only consider the polynomial dispersion relation $\Omega = \Omega_p = 8i\gamma\lambda^4\sigma - 2i\lambda^2\sigma$. From Eqs (2.2), (2.3), and (2.14), we have

$$\Psi_t = (8i\gamma\lambda^4 - 2i\lambda^2)\Psi R\sigma C_\lambda(\mathbb{I} - RC_\lambda)^{-1} - (8i\gamma\lambda^4 - 2i\lambda^2)\Psi\sigma(\mathbb{I} - RC_\lambda)^{-1} + (8i\gamma\lambda^4 - 2i\lambda^2)\Psi\sigma. \quad (2.16)$$

Then, through Eqs (2.9), Eq (2.16) can be written:

$$\begin{aligned} \Psi_t = & -8i\gamma[\sigma, \langle \lambda^3\Psi R \rangle]\Psi - 8i\gamma[\sigma, \langle \lambda^2\Psi R \rangle](\langle \Psi R \rangle + \lambda\mathbb{I})\Psi - 8i\gamma[\sigma, \langle \lambda\Psi R \rangle](\langle \lambda\Psi R \rangle + \langle \Psi R \rangle^2 + \lambda\langle \Psi R \rangle \\ & + \lambda^2\mathbb{I})\Psi - 8i\gamma[\sigma, \langle \Psi R \rangle](\langle \lambda^2\Psi R \rangle + \langle \lambda\Psi R \rangle\langle \Psi R \rangle + \lambda\langle \lambda\Psi R \rangle + \langle \Psi R \rangle\langle \lambda\Psi R \rangle + \langle \Psi R \rangle^3 + \lambda\langle \Psi R \rangle^2 \\ & + \lambda^2\langle \Psi R \rangle + \lambda^3\mathbb{I})\Psi - 8i\gamma\lambda^4[\sigma, \Psi] + 2i[\sigma, \langle \lambda\Psi R \rangle]\Psi + 2i\lambda^2[\sigma, \Psi] + 2i[\sigma, \langle \Psi R \rangle](\langle \Psi R \rangle + \lambda\mathbb{I})\Psi. \end{aligned} \quad (2.17)$$

Through Eqs (2.5) and (2.6), we get

$$\begin{aligned} \langle \Psi R \rangle_x &= i[\sigma, \langle \lambda\Psi R \rangle] + P\langle \Psi R \rangle, & \langle \lambda\Psi R \rangle_x &= i[\sigma, \langle \lambda^2\Psi R \rangle] + P\langle \lambda\Psi R \rangle, \\ \langle \lambda^2\Psi R \rangle_x &= i[\sigma, \langle \lambda^3\Psi R \rangle] + P\langle \lambda^2\Psi R \rangle. \end{aligned} \quad (2.18)$$

We decompose 4×4 matrix Q into $Q^{[o]}$ and $Q^{[d]}$ (i.e., $Q = Q^{[o]} + Q^{[d]}$), where $Q^{[o]}$ and $Q^{[d]}$ are expressed as

$$Q^{[o]} = \begin{pmatrix} 0 & Q_{12} & Q_{13} & Q_{14} \\ Q_{21} & 0 & 0 & 0 \\ Q_{31} & 0 & 0 & 0 \\ Q_{41} & 0 & 0 & 0 \end{pmatrix}, \quad Q^{[d]} = \begin{pmatrix} Q_{11} & 0 & 0 & 0 \\ 0 & Q_{22} & Q_{23} & Q_{24} \\ 0 & Q_{32} & Q_{33} & Q_{34} \\ 0 & Q_{42} & Q_{43} & Q_{44} \end{pmatrix}.$$

Therefore, from Eq (2.18), we obtain

$$\begin{aligned} \langle \Psi R \rangle_x^{[o]} &= 2i\sigma\langle \lambda\Psi R \rangle^{[o]} + P\langle \Psi R \rangle^{[d]}, & \langle \Psi R \rangle_x^{[d]} &= P\langle \Psi R \rangle^{[o]}, \\ \langle \lambda\Psi R \rangle_x^{[o]} &= 2i\sigma\langle \lambda^2\Psi R \rangle^{[o]} + P\langle \lambda\Psi R \rangle^{[d]}, & \langle \lambda\Psi R \rangle_x^{[d]} &= P\langle \lambda\Psi R \rangle^{[o]}, \\ \langle \lambda^2\Psi R \rangle_x^{[o]} &= 2i\sigma\langle \lambda^3\Psi R \rangle^{[o]} + P\langle \lambda^2\Psi R \rangle^{[d]}, & \langle \lambda^2\Psi R \rangle_x^{[d]} &= P\langle \lambda^2\Psi R \rangle^{[o]}. \end{aligned} \quad (2.19)$$

Based on Eqs (2.7) and (2.19), we have

$$\begin{aligned} 4\langle \lambda\Psi R \rangle^{[o]} &= -P_x + 2i\sigma P\langle \Psi R \rangle^{[d]}, \\ 8\langle \lambda^2\Psi R \rangle^{[o]} &= i\sigma P_{xx} + 4i\sigma P\langle \lambda\Psi R \rangle^{[d]} + 2P_x\langle \Psi R \rangle^{[d]} + 2P^2\langle \Psi R \rangle^{[o]}, \\ 16\langle \lambda^3\Psi R \rangle^{[o]} &= P_{xxx} + 8i\sigma P\langle \lambda^2\Psi R \rangle^{[d]} + 4P_x\langle \lambda\Psi R \rangle^{[d]} + 8P^2\langle \lambda\Psi R \rangle^{[o]} - 2i\sigma P_{xx}\langle \Psi R \rangle^{[d]} \\ &\quad - 4i\sigma P_x P\langle \Psi R \rangle^{[o]} - 2i\sigma P P_x\langle \Psi R \rangle^{[o]} - 2i\sigma P^3\langle \Psi R \rangle^{[d]}. \end{aligned} \quad (2.20)$$

Bringing (2.20) into Eq (2.17) yields Eq (2.15).

In conclusion, we derived that the solution Ψ of the $\bar{\partial}$ -problem (2.1) satisfies the time spectral problem.

3. Recursive operators and three-coupled fourth-order NLS hierarchy

In this section, in order to derive the three-coupled fourth-order NLS hierarchy, we first introduce a matrix function $M(x, t, \lambda)$, which is expressed as follows

$$M(x, t, \lambda) = \Psi \sigma \Psi^{-1}.$$

Letting $P = \begin{pmatrix} 0 & \bar{q}_1 & \bar{q}_2 & \bar{q}_3 \\ -q_1 & 0 & 0 & 0 \\ -q_2 & 0 & 0 & 0 \\ -q_3 & 0 & 0 & 0 \end{pmatrix}$, we can deduce the following proposition.

Proposition 3 *The matrix P defined in the Eq (2.7) satisfies a coupled hierarchy with a source $M(x, t, \lambda)$*

$$\begin{aligned} P_t + 2\alpha_n \sigma \Lambda^n P + 2\alpha_{n+2} \sigma \Lambda^{n+2} P &= -i[\sigma, \langle \omega(\lambda) M \rangle], \\ M_x &= i\lambda[\sigma, M] + [P, M], \end{aligned} \quad (3.1)$$

where the recursive operator Λ means it is defined as the following form

$$\Lambda = \frac{1}{2}i\sigma([P, \partial_x^{-1}[P, \cdot]] - \partial_x).$$

Remark 1 *For the special case of $n = 1$, we derive the generalized three-coupled third-order NLS equations with a source term from the coupled hierarchy equations (3.1). These equations are obtained as follows*

$$iq_{j,t} + \alpha_1 q_{j,x} - \frac{1}{4}\alpha_3 \left(q_{j,xxx} + 3 \sum_{\rho=1}^3 q_{\rho,x} \bar{q}_{\rho} q_j + 3 \sum_{\rho=1}^3 |q_{\rho}|^2 q_{j,x} \right) = -2\sigma \langle \omega(\lambda) M^{[o]} \rangle, \quad (j = 1, 2, 3),$$

$$\text{where } M = M^{[o]} + M^{[d]} = \begin{pmatrix} 0 & M_{12} & M_{13} & M_{14} \\ M_{21} & 0 & 0 & 0 \\ M_{31} & 0 & 0 & 0 \\ M_{41} & 0 & 0 & 0 \end{pmatrix} + \begin{pmatrix} M_{11} & 0 & 0 & 0 \\ 0 & M_{22} & M_{23} & M_{24} \\ 0 & M_{32} & M_{33} & M_{34} \\ 0 & M_{42} & Q_{43} & M_{44} \end{pmatrix}.$$

For $n = 2$, we derive the generalized three-coupled fourth-order NLS equations with a source term from the coupled hierarchy equations (3.1). These equations are obtained as follows

$$\begin{aligned} q_{j,t} + \frac{1}{2}\alpha_2 q_{j,xx} + \alpha_2 \sum_{\rho=1}^3 |q_{\rho}|^2 q_j - \frac{1}{8}\alpha_4 \left(q_{j,xxxx} + 6 \sum_{\rho=1}^3 q_{\rho,x} \bar{q}_{\rho} q_{j,x} + 2 \sum_{\rho=1}^3 |q_{\rho,x}|^2 q_j + 2 \sum_{\rho=1}^3 q_{\rho} \bar{q}_{\rho,x} q_{j,x} \right. \\ \left. + 4 \sum_{\rho=1}^3 |q_{\rho}|^2 q_{j,xx} + 4 \sum_{\rho=1}^3 q_{\rho,xx} \bar{q}_{\rho} q_j + 2 \sum_{\rho=1}^3 q_{\rho} \bar{q}_{\rho,xx} q_j + 6 \left(\sum_{\rho=1}^3 |q_{\rho}|^2 \right)^2 q_j \right) = 2i\sigma \langle \omega(\lambda) M^{[o]} \rangle, \quad (j = 1, 2, 3). \end{aligned} \quad (3.2)$$

By selecting $\alpha_2 = -2i$, $\alpha_4 = 8i\gamma$, and $\omega(\lambda) = 0$, Eqs (3.2) can be reduced to the three-coupled fourth-order NLS systems (1.1).

Proof According to the definition of C_{λ} and $A(\lambda) = \frac{1}{2\pi i} \frac{\partial}{\partial \lambda} \int \int_D \frac{A(\xi)}{\xi - \lambda} d\xi \wedge d\bar{\xi}$, we obtain the following result

$$\bar{\partial} f(\lambda) C_{\lambda} = \frac{1}{2\pi i} \frac{\partial}{\partial \bar{\lambda}} \int \int_D \frac{f(\xi)}{\xi - \lambda} d\xi \wedge d\bar{\xi} = f(\lambda),$$

where $\bar{\partial}$ can be interpreted as the inverse operator of C_λ . Therefore, we obtain

$$\langle (\Psi R)_t \rangle = \langle \Psi R_t, \mathbb{I} \cdot (\mathbb{I} + R^\top C_\lambda)^{-1} \rangle.$$

Making use of the relevant properties of Eq (2.4), and differentiating P with respect to t , yields the following result

$$P_t = i[\sigma, \langle \Psi R \rangle_t] = i[\sigma, \langle \Psi R_t, \mathbb{I} \cdot (\mathbb{I} + R^\top C_\lambda)^{-1} \rangle]. \quad (3.3)$$

Utilizing the identity $\bar{\partial}(\Psi^{-1})^\top = -(\Psi^{-1})^\top R^\top$, together with Eqs (2.2) and (2.3), leads to the following result

$$(\Psi^{-1})^\top = \mathbb{I} \cdot (\mathbb{I} + R^\top C_\lambda)^{-1}. \quad (3.4)$$

Then, by bringing Eqs (2.13) and (3.4) into Eq (3.3), we have

$$P_t = i[\sigma, \langle (\bar{\partial} \Psi) \Omega \Psi^{-1} \rangle] + i[\sigma, \langle \Psi \Omega \bar{\partial} \Psi^{-1} \rangle]. \quad (3.5)$$

Consider

$$\Omega_p = \alpha_n \lambda^n \sigma + \alpha_{n+2} \lambda^{n+2} \sigma,$$

and

$$\Omega_s \rightarrow 0, \quad \text{as } \lambda \rightarrow \infty.$$

Furthermore, Eq (3.5) can be simplified to

$$P_t = 2i\alpha_n \sigma \langle \bar{\partial}(\lambda^n M^{[o]}) \rangle + 2i\alpha_{n+2} \sigma \langle \bar{\partial}(\lambda^{n+2} M^{[o]}) \rangle - i[\sigma, \langle \omega(\lambda) M \rangle]. \quad (3.6)$$

Based on the definition of $M(x, t, \lambda)$, and with the aid of Eq (2.6), the second equation in Eq (3.1) is obtained.

Next, by substituting $M(x, t, \lambda) = M^{[o]}(x, t, \lambda) + M^{[d]}(x, t, \lambda)$ into the second equations of Eq (3.1), the following result is obtained

$$M_x^{[d]} = [P, M^{[o]}], \quad M_x^{[o]} = 2i\lambda \sigma M^{[o]} + [P, M^{[d]}]. \quad (3.7)$$

According to the boundary condition that $\Psi(x, t, \lambda) \rightarrow \mathbb{I}$ as $\lambda \rightarrow \infty$, we have

$$M(x, t, \lambda) = \Psi \sigma \Psi^{-1} \rightarrow \sigma, \quad \text{as } \lambda \rightarrow \infty,$$

and subsequently get the solution of $M^{[d]}$ to

$$M^{[d]} = \sigma + \partial_x^{-1} [P, M^{[o]}], \quad (3.8)$$

where ∂_x^{-1} represents the integral with respect to x . We bring Eq (3.8) into the second equation of Eq (3.7), and we obtain

$$\lambda M^{[o]} + \frac{i}{2} \sigma \left(M_x^{[o]} - [P, \partial_x^{-1} [P, M^{[o]}]] \right) = -iP.$$

Subsequently, the following new recursive operator is introduced

$$\Lambda = \frac{1}{2} i \sigma \left([P, \partial_x^{-1} [P, \cdot]] - \partial_x \right).$$

As a result, the following expression is obtained

$$M^{[o]} = i(\Lambda - \lambda)^{-1}P. \quad (3.9)$$

Substituting Eq (3.9) into Eq (3.6), we have

$$P_t = -2\alpha_n \sigma \langle \bar{\partial}(\lambda^n(\Lambda - \lambda)^{-1})P \rangle - 2\alpha_{n+2} \sigma \langle \bar{\partial}(\lambda^{n+2}(\Lambda - \lambda)^{-1})P \rangle - i[\sigma, \langle \omega(\lambda)M \rangle].$$

The expansion $(\Lambda - \lambda)^{-1} = -\sum_{j=1}^{\infty} \frac{\Lambda^{j-1}}{\lambda^j}$ is considered. Employing the identity $\bar{\partial}\lambda^{n-j} = \pi\delta(\lambda)\delta_{j,n+1}$ for $j = 1, 2, \dots$, the following result is derived

$$\langle \bar{\partial}\lambda^{n-j} \rangle = \frac{\delta_{j,n+1}}{2i} \int \int \delta(\lambda) d\lambda \wedge d\bar{\lambda} = -\delta_{j,n+1}.$$

As a consequence, the following evolution equation arises

$$P_t = -2\alpha_n \sigma \Lambda^n P - 2\alpha_{n+2} \sigma \Lambda^{n+2} P - i[\sigma, \langle \omega(\lambda)M \rangle].$$

4. The N -soliton solutions of the three-coupled fourth-order NLS system

In this section, we construct the N -soliton solution of the three-coupled fourth-order NLS systems (1.1) with the $\bar{\partial}$ -problem (2.1).

4.1. N -soliton solutions

Proposition 4 Suppose that $\lambda_j, \bar{\lambda}_j$ ($j = 1, 2, \dots, N$) are $2N$ discrete spectra in the complex plane. In the case of Eqs (2.5) and (2.13), we choose the spectral transform matrix as

$$R = \pi e^{-i\theta(\lambda)\sigma} \sum_{j=1}^N \mathfrak{R}_j e^{i\theta(\lambda)\sigma}, \quad (4.1)$$

where $\mathfrak{R}_j = \begin{pmatrix} 0 & -c_{1,j}\delta(\lambda - \lambda_j) & -c_{2,j}\delta(\lambda - \lambda_j) & -c_{3,j}\delta(\lambda - \lambda_j) \\ \bar{c}_{1,j}\delta(\lambda - \bar{\lambda}_j) & 0 & 0 & 0 \\ \bar{c}_{2,j}\delta(\lambda - \bar{\lambda}_j) & 0 & 0 & 0 \\ \bar{c}_{3,j}\delta(\lambda - \bar{\lambda}_j) & 0 & 0 & 0 \end{pmatrix}$, $\theta(\lambda) = -\lambda x + (8\gamma\lambda^4 - 2\lambda^2)t$, $c_{h,j}, \bar{c}_{h,j}$ ($h = 1, 2, 3$, $j = 1, 2, \dots, N$) are all constants. Based on Eqs (2.7) and (4.1), we derive the N -soliton solutions of the three-coupled fourth-order NLS systems (1.1) as

$$q_1 = \overline{\left(-2i \frac{\det M^{(1)}}{\det M} \right)}, \quad q_2 = \overline{\left(-2i \frac{\det M^{(2)}}{\det M} \right)}, \quad q_3 = \overline{\left(-2i \frac{\det M^{(3)}}{\det M} \right)}, \quad (4.2)$$

where

$$M^{(1)} = \begin{pmatrix} 0 & K_{1N} \\ E & M \end{pmatrix}, \quad M^{(2)} = \begin{pmatrix} 0 & K_{2N} \\ E & M \end{pmatrix}, \quad M^{(3)} = \begin{pmatrix} 0 & K_{3N} \\ E & M \end{pmatrix},$$

$$E = (1, 1, \dots, 1)_{1 \times N}^T, \quad K_{1N} = (c_{1,1}e^{-2i\theta(\lambda_1)}, c_{1,2}e^{-2i\theta(\lambda_2)}, \dots, c_{1,N}e^{-2i\theta(\lambda_N)})_{1 \times N},$$

$$K_{2N} = (c_{2,1}e^{-2i\theta(\lambda_1)}, c_{2,2}e^{-2i\theta(\lambda_2)}, \dots, c_{2,N}e^{-2i\theta(\lambda_N)})_{1 \times N},$$

$$K_{3N} = (c_{3,1}e^{-2i\theta(\lambda_1)}, c_{3,2}e^{-2i\theta(\lambda_2)}, \dots, c_{3,N}e^{-2i\theta(\lambda_N)})_{1 \times N}.$$

Proof Based on Eqs (2.7) and (4.1), the following result is obtained

$$\begin{aligned} q_1(x, t) &= \overline{\left(2i \sum_{j=1}^N c_{1,j} e^{-2i\theta(\lambda_j)} \Psi_{11}(\lambda_j)\right)}, & q_2(x, t) &= \overline{\left(2i \sum_{j=1}^N c_{2,j} e^{-2i\theta(\lambda_j)} \Psi_{11}(\lambda_j)\right)}, \\ q_3(x, t) &= \overline{\left(2i \sum_{j=1}^N c_{3,j} e^{-2i\theta(\lambda_j)} \Psi_{11}(\lambda_j)\right)}. \end{aligned} \quad (4.3)$$

Substituting Eq (4.1) into Eq (2.2), we get

$$\Psi_{11}(\lambda) = 1 + \sum_{j=1}^N \left(\frac{\bar{c}_{1,j} e^{2i\theta(\bar{\lambda}_j)} \Psi_{12}(\bar{\lambda}_j) + \bar{c}_{2,j} e^{2i\theta(\bar{\lambda}_j)} \Psi_{13}(\bar{\lambda}_j) + \bar{c}_{3,j} e^{2i\theta(\bar{\lambda}_j)} \Psi_{14}(\bar{\lambda}_j)}{\lambda - \bar{\lambda}_j} \right), \quad (4.4)$$

$$\begin{aligned} \Psi_{12}(\lambda) &= - \sum_{k=1}^N \left(\frac{c_{1,k} e^{-2i\theta(\lambda_k)} \Psi_{11}(\lambda_k)}{\lambda - \lambda_k} \right), & \Psi_{13}(\lambda) &= - \sum_{k=1}^N \left(\frac{c_{2,k} e^{-2i\theta(\lambda_k)} \Psi_{11}(\lambda_k)}{\lambda - \lambda_k} \right), \\ \Psi_{14}(\lambda) &= - \sum_{k=1}^N \left(\frac{c_{3,k} e^{-2i\theta(\lambda_k)} \Psi_{11}(\lambda_k)}{\lambda - \lambda_k} \right). \end{aligned} \quad (4.5)$$

We assume

$$A_j = \frac{\bar{c}_{1,j}}{\lambda - \bar{\lambda}_j} e^{2i\theta(\bar{\lambda}_j)}, \quad B_j = \frac{\bar{c}_{2,j}}{\lambda - \bar{\lambda}_j} e^{2i\theta(\bar{\lambda}_j)}, \quad C_j = \frac{\bar{c}_{3,j}}{\lambda - \bar{\lambda}_j} e^{2i\theta(\bar{\lambda}_j)},$$

and taking $\lambda = \lambda_n$ in Eq (4.4), $\lambda = \bar{\lambda}_n$ in Eqs (4.5). Therefore, we rewrite Eqs (4.4) and (4.5) as

$$\begin{aligned} \Psi_{11}(\lambda_n) &= 1 + \sum_{j=1}^N A_j(\lambda_n) \Psi_{12}(\bar{\lambda}_j) + \sum_{j=1}^N B_j(\lambda_n) \Psi_{13}(\bar{\lambda}_j) + \sum_{j=1}^N C_j(\lambda_n) \Psi_{14}(\bar{\lambda}_j), \\ \Psi_{12}(\bar{\lambda}_j) &= - \sum_{k=1}^N \overline{A_k(\bar{\lambda}_j)} \Psi_{11}(\lambda_k), \quad \Psi_{13}(\bar{\lambda}_j) = - \sum_{k=1}^N \overline{B_k(\bar{\lambda}_j)} \Psi_{11}(\lambda_k), \quad \Psi_{14}(\bar{\lambda}_j) = - \sum_{k=1}^N \overline{C_k(\bar{\lambda}_j)} \Psi_{11}(\lambda_k). \end{aligned}$$

Furthermore, the following result is obtained

$$\Psi_{11}(\lambda_n) = 1 - \sum_{j=1}^N \sum_{k=1}^N \left(A_j(\lambda_n) \overline{A_k(\bar{\lambda}_j)} + B_j(\lambda_n) \overline{B_k(\bar{\lambda}_j)} + C_j(\lambda_n) \overline{C_k(\bar{\lambda}_j)} \right) \Psi_{11}(\lambda_k), \quad (n = 1, 2, \dots, N). \quad (4.6)$$

We rewrite Eq (4.6) as

$$M(\Psi_{11}(\lambda_1), \Psi_{11}(\lambda_2), \dots, \Psi_{11}(\lambda_N))^T = (1, 1, \dots, 1)^T, \quad (4.7)$$

where M means the $N \times N$ matrix,

$$M = \mathbb{I} + F_{n,k}, \quad F_{n,k} = \sum_{j=1}^N \left(A_j(\lambda_n) \overline{A_k(\bar{\lambda}_j)} + B_j(\lambda_n) \overline{B_k(\bar{\lambda}_j)} + C_j(\lambda_n) \overline{C_k(\bar{\lambda}_j)} \right).$$

By solving Eq (4.7), we can get

$$\Psi_{11}(\lambda_n) = \frac{\det M_n^r}{\det M}, \quad (n = 1, 2, \dots, N), \quad (4.8)$$

with $M_n^r = (M_1, \dots, M_{n-1}, E, M_{n+1}, \dots, M_N)$. We bring Eq (4.8) into Eq (4.3) and get the N -soliton solutions of the three-coupled fourth-order NLS systems (1.1).

4.2. Application of N -soliton solutions

4.2.1. 1-soliton solutions

First of all, we consider the 1-soliton solution, and assume that $N = 1$. According to the definition of M , we have

$$M = 1 + A_1(\lambda) \overline{A_1(\bar{\lambda})} + B_1(\lambda) \overline{B_1(\bar{\lambda})} + C_1(\lambda) \overline{C_1(\bar{\lambda})},$$

$$M^{(1)} = \begin{pmatrix} 0 & c_{1,1} e^{-2i\theta(\lambda)} \\ 1 & M \end{pmatrix}, \quad M^{(2)} = \begin{pmatrix} 0 & c_{2,1} e^{-2i\theta(\lambda)} \\ 1 & M \end{pmatrix}, \quad M^{(3)} = \begin{pmatrix} 0 & c_{3,1} e^{-2i\theta(\lambda)} \\ 1 & M \end{pmatrix}.$$

From Eq (4.2), we can get the 1-soliton solutions of the three-coupled fourth-order NLS systems (1.1) as

$$\begin{aligned} q_1(x, t) &= \frac{2ic_{1,1}e^{2i(\lambda x - 8\gamma\lambda^4 t + 2\lambda^2 t)}(\lambda - \bar{\lambda})(\bar{\lambda} - \lambda)}{(\lambda - \bar{\lambda})(\bar{\lambda} - \lambda) + (c_{1,1}\bar{c}_{1,1} + c_{2,1}\bar{c}_{2,1} + c_{3,1}\bar{c}_{3,1})e^{2i(-\bar{\lambda}x + 8\gamma\bar{\lambda}^4 t - 2\bar{\lambda}^2 t + \lambda x - 8\gamma\lambda^4 t + 2\lambda^2 t)}} \\ &= -ic_{1,1}e^{-iH - \varrho_1 - i\varrho_2} \operatorname{sech}(iG + \varrho_1 + i\varrho_2), \\ q_2(x, t) &= \frac{2ic_{2,1}e^{2i(\lambda x - 8\gamma\lambda^4 t + 2\lambda^2 t)}(\lambda - \bar{\lambda})(\bar{\lambda} - \lambda)}{(\lambda - \bar{\lambda})(\bar{\lambda} - \lambda) + (c_{1,1}\bar{c}_{1,1} + c_{2,1}\bar{c}_{2,1} + c_{3,1}\bar{c}_{3,1})e^{2i(-\bar{\lambda}x + 8\gamma\bar{\lambda}^4 t - 2\bar{\lambda}^2 t + \lambda x - 8\gamma\lambda^4 t + 2\lambda^2 t)}} \\ &= -ic_{2,1}e^{-iH - \varrho_1 - i\varrho_2} \operatorname{sech}(iG + \varrho_1 + i\varrho_2), \\ q_3(x, t) &= \frac{2ic_{3,1}e^{2i(\lambda x - 8\gamma\lambda^4 t + 2\lambda^2 t)}(\lambda - \bar{\lambda})(\bar{\lambda} - \lambda)}{(\lambda - \bar{\lambda})(\bar{\lambda} - \lambda) + (c_{1,1}\bar{c}_{1,1} + c_{2,1}\bar{c}_{2,1} + c_{3,1}\bar{c}_{3,1})e^{2i(-\bar{\lambda}x + 8\gamma\bar{\lambda}^4 t - 2\bar{\lambda}^2 t + \lambda x - 8\gamma\lambda^4 t + 2\lambda^2 t)}} \\ &= -ic_{3,1}e^{-iH - \varrho_1 - i\varrho_2} \operatorname{sech}(iG + \varrho_1 + i\varrho_2), \end{aligned} \quad (4.9)$$

where

$$H = 2(\lambda^2 - 4\gamma\lambda^4 + \bar{\lambda}^2 - 4\gamma\bar{\lambda}^4)t + (\lambda + \bar{\lambda})x, \quad G = 2(\lambda^2 - 4\gamma\lambda^4 - \bar{\lambda}^2 + 4\gamma\bar{\lambda}^4)t + (\lambda - \bar{\lambda})x.$$

Next, we assume $\lambda = \zeta_1 + i\zeta_2$ and simplify Eq (4.9) to

$$\begin{aligned} q_1(x, t) &= -ic_{1,1}e^{\nu_1(x,t)} \operatorname{sech}(\nu_2(x, t)), \\ q_2(x, t) &= -ic_{2,1}e^{\nu_1(x,t)} \operatorname{sech}(\nu_2(x, t)), \\ q_3(x, t) &= -ic_{3,1}e^{\nu_1(x,t)} \operatorname{sech}(\nu_2(x, t)), \end{aligned} \quad (4.10)$$

where

$$\begin{aligned} \nu_1(x, t) &= 4i(4\zeta_1^4\gamma - 24\zeta_1^2\zeta_2^2\gamma + 4\zeta_2^4\gamma - \zeta_1^2 + \zeta_2^2) - 2i\zeta_1 x - \varrho_1 - i\varrho_2, \\ \nu_2(x, t) &= 8(8\zeta_1^3\zeta_2\gamma - 8\zeta_1\zeta_2^3\gamma - \zeta_1\zeta_2)t - 2\zeta_2 x + \varrho_1 + i\varrho_2. \end{aligned}$$

From the explicit one-soliton expression, the phase function $\nu_1(x, t)$ shows that the oscillation periods in x and t can be obtained from the argument of the exponential term $e^{\nu_1(x,t)}$. Accordingly, the time period T_t and spatial period T_x can be approximated as

$$T_t = \frac{\pi}{|4\zeta_1(\zeta^2 - 6\beta^2)\gamma - \frac{1}{2}\zeta|}, \quad T_x = \frac{\pi}{|\zeta|}.$$

These periods depend on the real part ζ of the spectral parameter and on the higher-order coupling coefficient γ .

We analyze the characteristic lines associated with Eq (4.10), which describe the dynamics of the soliton solutions. In particular, we identify a characteristic line $L_1 : v_2(x, t) = 0$, which corresponds to the propagation path of the 1-soliton solution. The function $v_2(x, t)$ originally serves to define this characteristic line; however, since $v_2(x, t)$ generally contains complex-valued terms, it does not directly represent a physically meaningful (i.e., real-valued) trajectory in the (x, t) -plane.

To better understand the actual motion of the soliton, we focus on the real part of the phase function $v_2(x, t)$. By isolating the linear terms in x and t from $\Re(v_2(x, t))$, we obtain a real-valued approximation of the characteristic line that captures the soliton's dominant propagation direction. These linear components provide insight into the soliton's trajectory and are used to plot the characteristic line. The effect of different parameter choices on this characteristic path is illustrated in Figure 1(d) and 2(d), where variations in slope and position reflect changes in soliton velocity and initial phase.

By selecting appropriate parameter values, the dynamic behavior of the 1-soliton solutions are illustrated in Figures 1 and 2. It is observed that the width and amplitude of a single soliton remain invariant during propagation. Moreover, singularities in the soliton profiles are located along the corresponding characteristic lines. A comparison between Figures 1 and 2 further reveals that variations in the real part of the discrete spectral parameter lead to oscillatory behavior in the wave.

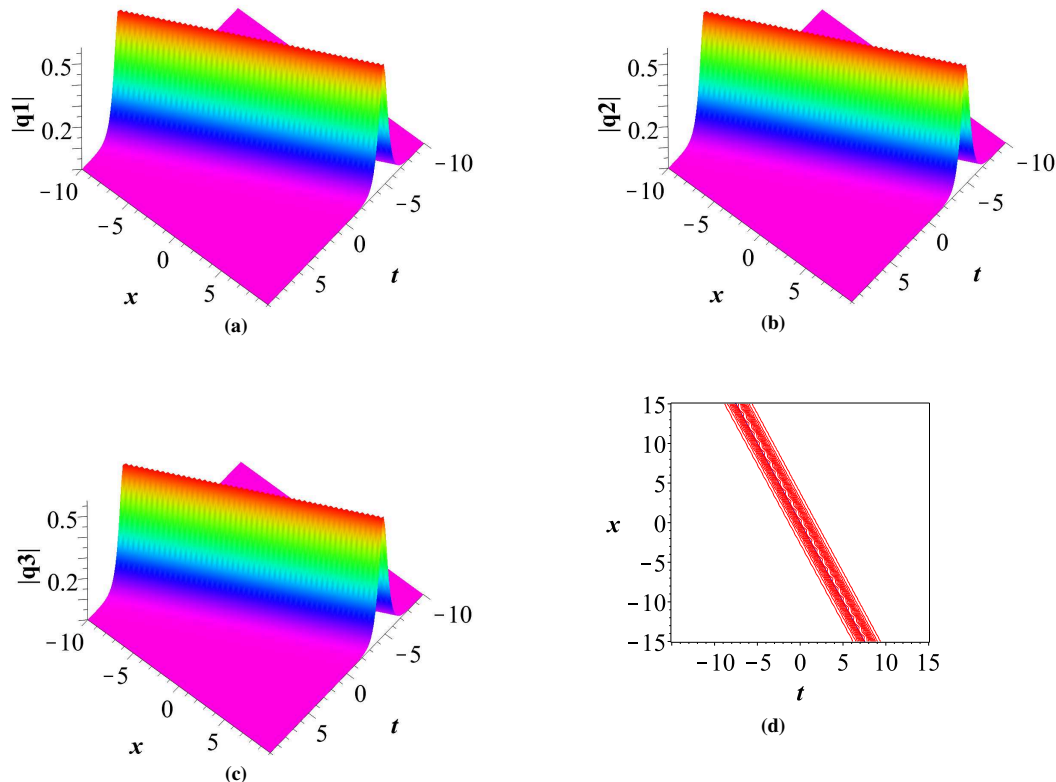


Figure 1. The 1-soliton solution (4.10) for Eq (1.1) with the parameters $\zeta_1 = \frac{1}{2}$, $\zeta_2 = \frac{1}{2}$, $c_{1,1} = 1$, $c_{2,1} = 1$, $c_{3,1} = 1$, and $\gamma = 4$; (a) Three-dimensional plot of q_1 ; (b) Three-dimensional plot of q_2 ; (c) Three-dimensional plot of q_3 ; (d) The characteristic line $L_1 : x = -2t$.

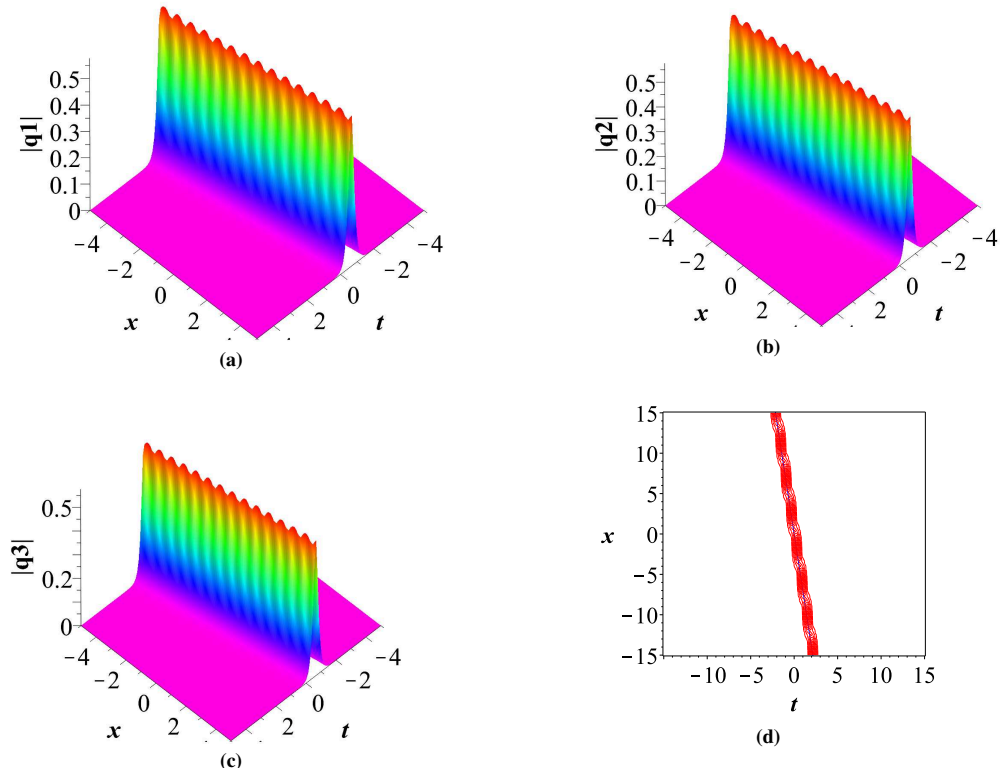


Figure 2. The 1-soliton solution (4.10) for Eq (1.1) with the parameters $\zeta_1 = \frac{1}{4}$, $\zeta_2 = \frac{1}{2}$, $c_{1,1} = 1$, $c_{2,1} = 1$, $c_{3,1} = 1$, and $\gamma = 4$; (a) Three-dimensional plot of q_1 ; (b) Three-dimensional plot of q_2 ; (c) Three-dimensional plot of q_3 ; (d) The characteristic line $L_1 : x = -\frac{196}{27}t$.

4.2.2. 2-soliton solutions

Assuming $N = 2$, and then using the definition of M , we have

$$M = \begin{pmatrix} M_{11} & M_{12} \\ M_{21} & M_{22} \end{pmatrix},$$

$$M^{(1)} = \begin{pmatrix} 0 & c_{1,1}e^{-2i\theta(\lambda_1)} & c_{1,2}e^{-2i\theta(\lambda_2)} \\ 1 & M_{11} & M_{12} \\ 1 & M_{21} & M_{22} \end{pmatrix}, \quad M^{(2)} = \begin{pmatrix} 0 & c_{2,1}e^{-2i\theta(\lambda_1)} & c_{2,2}e^{-2i\theta(\lambda_2)} \\ 1 & M_{11} & M_{12} \\ 1 & M_{21} & M_{22} \end{pmatrix},$$

$$M^{(3)} = \begin{pmatrix} 0 & c_{3,1}e^{-2i\theta(\lambda_1)} & c_{3,2}e^{-2i\theta(\lambda_2)} \\ 1 & M_{11} & M_{12} \\ 1 & M_{21} & M_{22} \end{pmatrix},$$

where

$$\begin{aligned}
M_{11} &= 1 + A_1(\lambda_1)\overline{A_1(\bar{\lambda}_1)} + B_1(\lambda_1)\overline{B_1(\bar{\lambda}_1)} + C_1(\lambda_1)\overline{C_1(\bar{\lambda}_1)} \\
&\quad + A_2(\lambda_1)\overline{A_1(\bar{\lambda}_2)} + B_2(\lambda_1)\overline{B_1(\bar{\lambda}_2)} + C_2(\lambda_1)\overline{C_1(\bar{\lambda}_2)}, \\
M_{12} &= A_1(\lambda_1)\overline{A_2(\bar{\lambda}_1)} + B_1(\lambda_1)\overline{B_2(\bar{\lambda}_1)} + C_1(\lambda_1)\overline{C_2(\bar{\lambda}_1)} \\
&\quad + A_2(\lambda_1)\overline{A_2(\bar{\lambda}_2)} + B_2(\lambda_1)\overline{B_2(\bar{\lambda}_2)} + C_2(\lambda_1)\overline{C_2(\bar{\lambda}_2)}, \\
M_{21} &= A_1(\lambda_2)\overline{A_1(\bar{\lambda}_1)} + B_1(\lambda_2)\overline{B_1(\bar{\lambda}_1)} + C_1(\lambda_2)\overline{C_1(\bar{\lambda}_1)} \\
&\quad + A_2(\lambda_2)\overline{A_1(\bar{\lambda}_2)} + B_2(\lambda_2)\overline{B_1(\bar{\lambda}_2)} + C_2(\lambda_2)\overline{C_1(\bar{\lambda}_2)}, \\
M_{22} &= 1 + A_1(\lambda_2)\overline{A_2(\bar{\lambda}_1)} + B_1(\lambda_2)\overline{B_2(\bar{\lambda}_1)} + C_1(\lambda_2)\overline{C_2(\bar{\lambda}_1)} \\
&\quad + A_2(\lambda_2)\overline{A_2(\bar{\lambda}_2)} + B_2(\lambda_2)\overline{B_2(\bar{\lambda}_2)} + C_2(\lambda_2)\overline{C_2(\bar{\lambda}_2)}.
\end{aligned}$$

Therefore, we conclude that the 2-soliton solutions of the three-coupled fourth-order NLS systems (1.1) can be described as follows

$$q_1 = \overline{\left(-2i \frac{\det M^{(1)}}{\det M} \right)}, \quad q_2 = \overline{\left(-2i \frac{\det M^{(2)}}{\det M} \right)}, \quad q_3 = \overline{\left(-2i \frac{\det M^{(3)}}{\det M} \right)}. \quad (4.11)$$

By setting $N = 2$ in the general N -soliton expression (4.2), we obtain the 2-soliton solutions of the three-coupled fourth-order NLS system (1.1). Although the full analytic expressions are not shown due to their complexity, we visualize the solution in Figures 3–7 by selecting specific parameter values to illustrate the soliton interactions.

In addition, following the same approach used for the 1-soliton solutions, we assume $\lambda_1 = \zeta_1 + i\beta_1$ and $\lambda_2 = \zeta_2 + i\beta_2$. Under this assumption, we derive that the 2-soliton solutions possess the following two characteristic lines

$$\begin{aligned}
L_1 : \beta_1 x + 4(8\zeta_1\beta_1^3\gamma - 8\zeta_1^3\beta_1\gamma + \zeta_1\beta_1)t - \frac{1}{2\beta_1} \ln(c_{1,1}\bar{c}_{1,1} + c_{2,1}\bar{c}_{2,1} + c_{3,1}\bar{c}_{3,1}) &= 0, \\
L_2 : \beta_2 x + 4(8\zeta_2\beta_2^3\gamma - 8\zeta_2^3\beta_2\gamma + \zeta_2\beta_2)t - \frac{1}{2\beta_2} \ln(c_{1,2}\bar{c}_{1,2} + c_{2,2}\bar{c}_{2,2} + c_{3,2}\bar{c}_{3,2}) &= 0.
\end{aligned}$$

Figures 3–7 illustrate various 2-soliton interaction scenarios of the coupled fourth-order NLS systems by employing different configurations of the discrete spectral parameters ζ_j , β_j , and corresponding polarization components $c_{i,j}$. These simulations serve to highlight how specific spectral choices influence the interaction types, degrees of deformation, and propagation geometry of the solitons.

In Figures 3 and 4, the parameters $\zeta_1 = -\frac{1}{4}$, $\zeta_2 = \frac{1}{4}$ and $\zeta_1 = -\frac{11}{24}$, $\zeta_2 = \frac{15}{48}$, respectively, ensure that the two solitons possess distinct velocities and moderate spectral separation. As a result, the solitons exhibit elastic collisions, characterized by a brief nonlinear interaction and a subsequent restoration of their initial shapes and velocities. The characteristic lines L_1 and L_2 further confirm that the trajectories intersect but then diverge, indicating no permanent deformation or energy trapping.

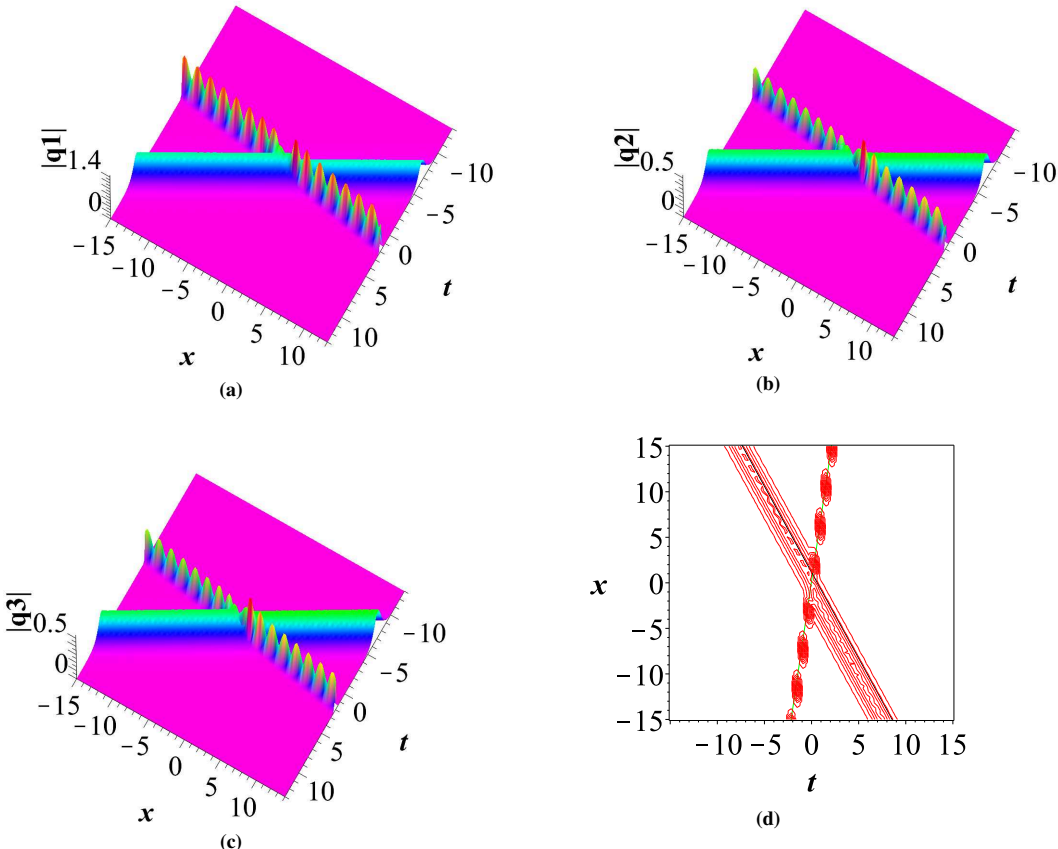


Figure 3. The 2-soliton solution (4.11) for Eq (1.1) with the parameters $\zeta_1 = -\frac{1}{2}$, $\beta_1 = \frac{3}{4}$, $\zeta_2 = \frac{1}{4}$, $\beta_2 = \frac{5}{12}$, $c_{1,1} = 1$, $c_{1,2} = 1$, $c_{2,1} = \frac{1}{3}$, $c_{2,2} = \frac{1}{2}$, $c_{3,1} = \frac{1}{3}$, $c_{3,2} = \frac{1}{2}$, and $\gamma = 1$; (a) Three-dimensional plot of q_1 ; (b) Three-dimensional plot of q_2 ; (c) Three-dimensional plot of q_3 ; (d) The characteristic line $L_1 : x = 7t + \frac{8}{9} \ln(\frac{11}{9})$ and $L_2 : x = -\frac{17}{9}t + \frac{72}{25} \ln(\frac{3}{2})$.

In Figure 5, the condition $\zeta_1 = -\frac{1}{2}$, $\zeta_2 = \frac{1}{4}$ with identical imaginary parts and smaller spectral separation results in a more intense interaction. Notably, the two solitons temporarily merge into a high-amplitude, signaling a singular behavior. This effect stems from constructive interference due to matching propagation velocities and overlapping phases, which can be interpreted physically as a momentary energy concentration or soliton fusion.

A comparative analysis of Figures 3–5 reveals that as the distance between the discrete eigenvalues decreases in terms of either the real or imaginary parts the interaction becomes stronger and longer in duration. This highlights the sensitivity of nonlinear superposition to spectral proximity, especially in coupled systems.

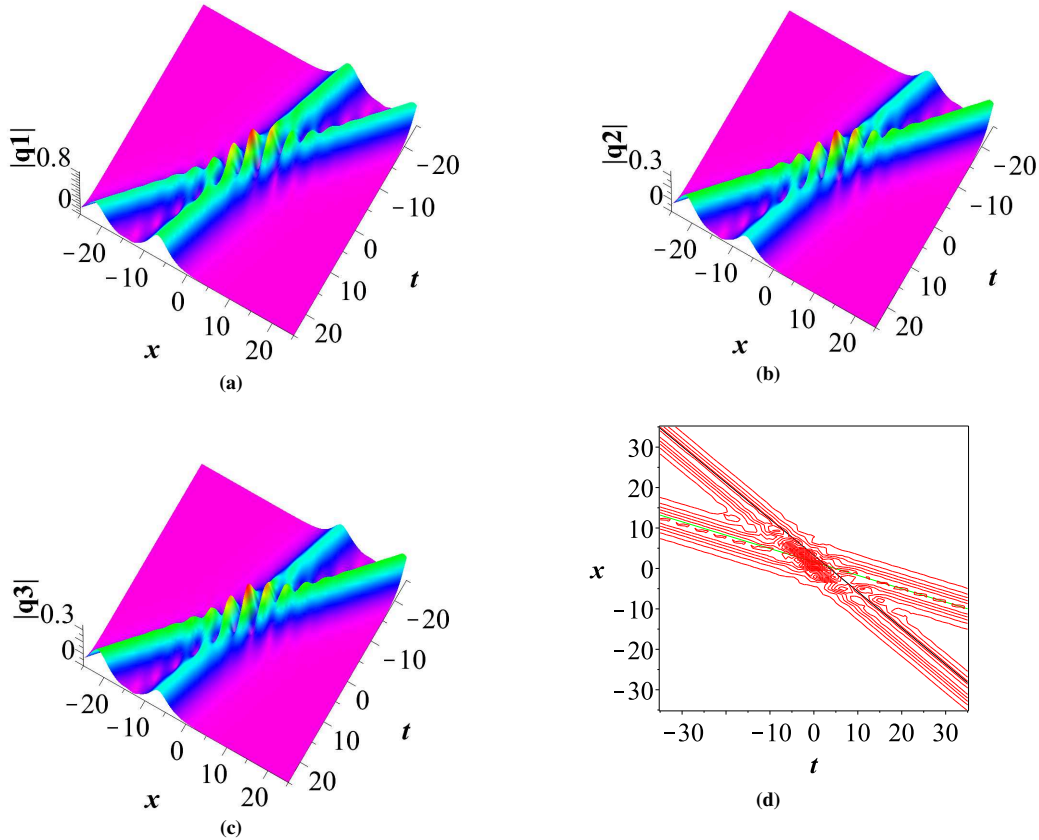


Figure 4. The 2-soliton solution (4.11) for Eq (1.1) with the parameters $\zeta_1 = -\frac{11}{24}$, $\beta_1 = \frac{1}{4}$, $\zeta_2 = \frac{15}{48}$, $\beta_2 = \frac{1}{4}$, $c_{1,1} = 1$, $c_{1,2} = 1$, $c_{2,1} = \frac{1}{3}$, $c_{2,2} = \frac{1}{2}$, $c_{3,1} = \frac{1}{3}$, $c_{3,2} = \frac{1}{2}$, and $\gamma = 1$; (a) Three-dimensional plot of q_1 ; (b) Three-dimensional plot of q_2 ; (c) Three-dimensional plot of q_3 ; (d) The characteristic line $L_1 : x = -\frac{143}{432}t + 8 \ln(\frac{11}{9})$ and $L_2 : x = -\frac{115}{128}t + 8 \ln(\frac{3}{2})$.

Figures 6 and 7 explore a symmetric setting with parameters $\zeta_1 = -\zeta_2 = \mp\frac{7}{24}$, $\beta_1 = -\beta_2 = \mp\frac{7}{24}$ corresponding to solitons with equal and opposite velocities. The characteristic lines L_1 and L_2 in these cases are symmetric and perpendicular, which geometrically implies that the solitons travel in mirror-opposite directions. Despite the head-on collision, the solitons retain their shape and energy, further reinforcing the elastic nature of these interactions. Interestingly, by comparing subfigures 6(d) and 7(d), we observe that rotating the characteristic lines by equal angles leads to a rotation in the interaction frame, but does not affect the qualitative soliton behavior and only their direction of motion is altered.

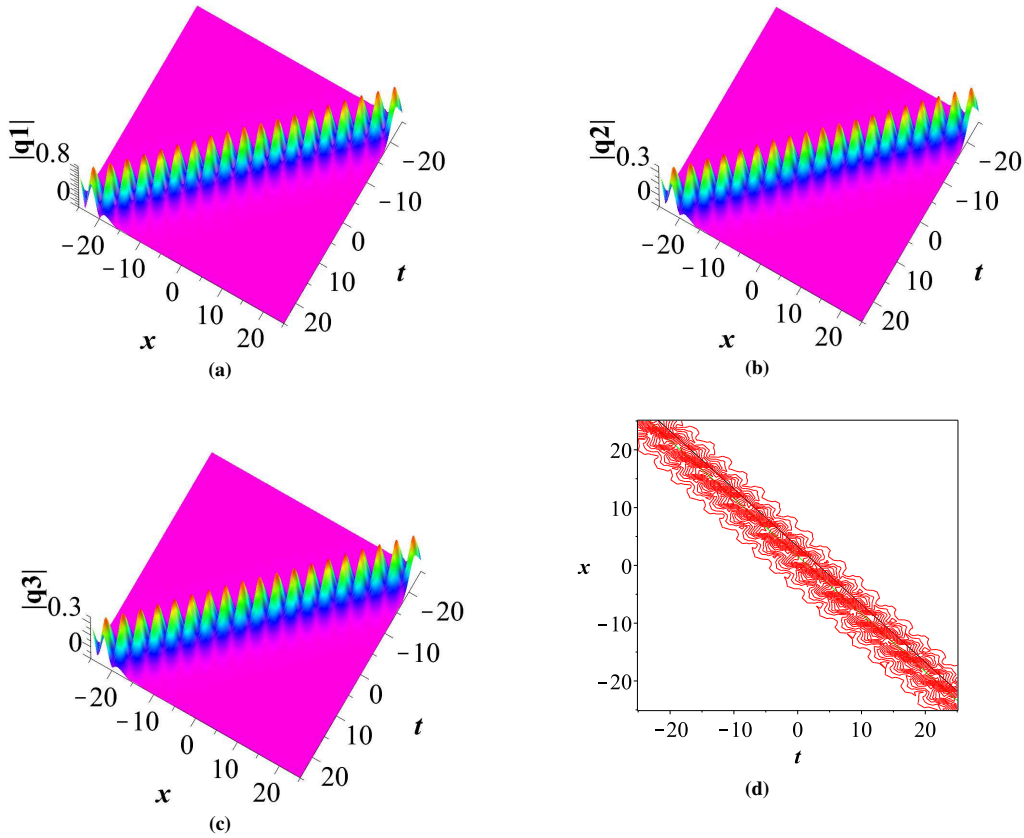


Figure 5. The 2-soliton solution (4.11) for Eq (1.1) with the parameters $\zeta_1 = -\frac{1}{2}$, $\beta_1 = \frac{1}{4}$, $\zeta_2 = \frac{1}{4}$, $\beta_2 = \frac{1}{4}$, $c_{1,1} = 1$, $c_{1,2} = 1$, $c_{2,1} = \frac{1}{3}$, $c_{2,2} = \frac{1}{2}$, $c_{3,1} = \frac{1}{3}$, $c_{3,2} = \frac{1}{2}$, and $\gamma = 1$; (a) Three-dimensional plot of q_1 ; (b) Three-dimensional plot of q_2 ; (c) Three-dimensional plot of q_3 ; (d) The characteristic line $L_1 : x = -t + 8 \ln(\frac{11}{9})$ and $L_2 : x = -t + 8 \ln(\frac{3}{2})$.

From a physical perspective, these interaction behaviors carry significance in various nonlinear media where multi-component soliton dynamics are present, such as optical fiber arrays, plasma waves, or multi-mode Bose-Einstein condensates. The observed elastic and singular interactions may correspond to stable transmission channels, energy localization, or directional switching mechanisms, which have practical applications in signal processing and nonlinear control systems.

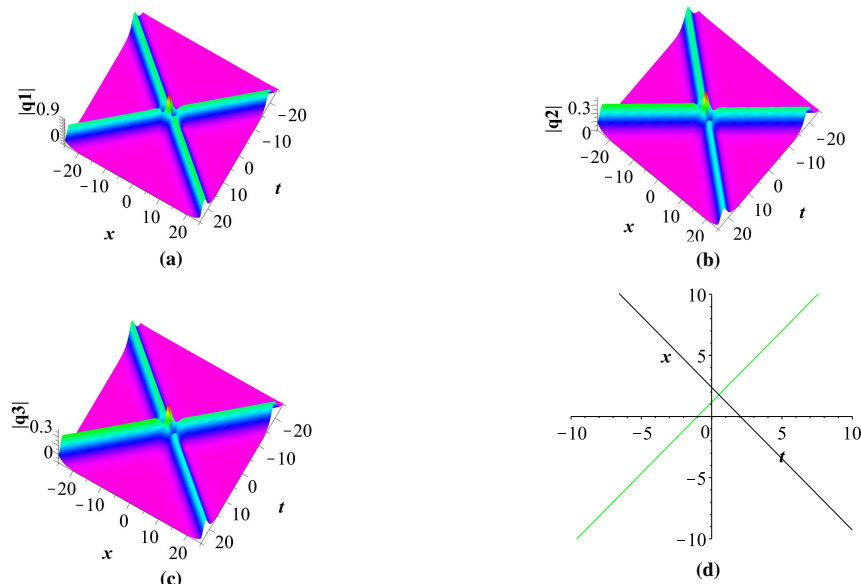


Figure 6. The 2-soliton solution (4.11) for Eq (1.1) with the parameters $\zeta_1 = -\frac{7}{24}$, $\beta_1 = -\frac{7}{24}$, $\zeta_2 = \frac{7}{24}$, $\beta_2 = \frac{7}{24}$, $c_{1,1} = 1$, $c_{1,2} = 1$, $c_{2,1} = \frac{1}{3}$, $c_{2,2} = \frac{1}{2}$, $c_{3,1} = \frac{1}{3}$, $c_{3,2} = \frac{1}{2}$, and $\gamma = 1$; (a) Three-dimensional plot of q_1 ; (b) Three-dimensional plot of q_2 ; (c) Three-dimensional plot of q_3 ; (d) The characteristic line $L_1 : x = \frac{7}{6}t + \frac{288}{49} \ln(\frac{11}{9})$ and $L_2 : x = -\frac{7}{6}t + \frac{288}{49} \ln(\frac{3}{2})$.

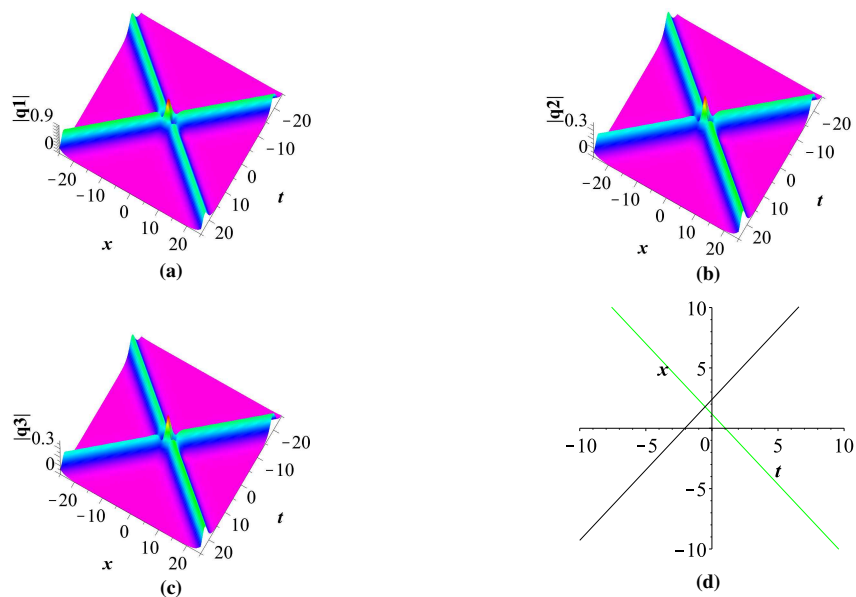


Figure 7. The 2-soliton solution (4.11) for Eq (1.1) with the parameters $\zeta_1 = \frac{7}{24}$, $\beta_1 = \frac{7}{24}$, $\zeta_2 = -\frac{7}{24}$, $\beta_2 = -\frac{7}{24}$, $c_{1,1} = 1$, $c_{1,2} = 1$, $c_{2,1} = \frac{1}{3}$, $c_{2,2} = \frac{1}{2}$, $c_{3,1} = \frac{1}{3}$, $c_{3,2} = \frac{1}{2}$, and $\gamma = 1$; (a) Three-dimensional plot of q_1 ; (b) Three-dimensional plot of q_2 ; (c) Three-dimensional plot of q_3 ; (d) The characteristic line $L_1 : x = -\frac{7}{6}t + \frac{288}{49} \ln(\frac{11}{9})$ and $L_2 : x = \frac{7}{6}t + \frac{288}{49} \ln(\frac{3}{2})$.

4.2.3. 3-soliton solutions

Assuming $N = 3$, and then using the definition of M , we obtain

$$M = \begin{pmatrix} M_{11} & M_{12} & M_{13} \\ M_{21} & M_{22} & M_{23} \\ M_{31} & M_{32} & M_{33} \end{pmatrix}, \quad M^{(1)} = \begin{pmatrix} 0 & c_{1,1}e^{-2i\theta(\lambda_1)} & c_{1,2}e^{-2i\theta(\lambda_2)} & c_{1,3}e^{-2i\theta(\lambda_3)} \\ 1 & M_{11} & M_{12} & M_{13} \\ 1 & M_{21} & M_{22} & M_{23} \\ 1 & M_{31} & M_{32} & M_{33} \end{pmatrix},$$

$$M^{(2)} = \begin{pmatrix} 0 & c_{2,1}e^{-2i\theta(\lambda_1)} & c_{2,2}e^{-2i\theta(\lambda_2)} & c_{2,3}e^{-2i\theta(\lambda_3)} \\ 1 & M_{11} & M_{12} & M_{13} \\ 1 & M_{21} & M_{22} & M_{23} \\ 1 & M_{31} & M_{32} & M_{33} \end{pmatrix},$$

$$M^{(3)} = \begin{pmatrix} 0 & c_{3,1}e^{-2i\theta(\lambda_1)} & c_{3,2}e^{-2i\theta(\lambda_2)} & c_{3,3}e^{-2i\theta(\lambda_3)} \\ 1 & M_{11} & M_{12} & M_{13} \\ 1 & M_{21} & M_{22} & M_{23} \\ 1 & M_{31} & M_{32} & M_{33} \end{pmatrix},$$

where

$$M_{11} = A_1(\lambda_1)\overline{A_1(\bar{\lambda}_1)} + B_1(\lambda_1)\overline{B_1(\bar{\lambda}_1)} + C_1(\lambda_1)\overline{C_1(\bar{\lambda}_1)} + A_2(\lambda_1)\overline{A_1(\bar{\lambda}_2)} + B_2(\lambda_1)\overline{B_1(\bar{\lambda}_2)} \\ + C_2(\lambda_1)\overline{C_1(\bar{\lambda}_2)} + A_3(\lambda_1)\overline{A_1(\bar{\lambda}_3)} + B_3(\lambda_1)\overline{B_1(\bar{\lambda}_3)} + C_3(\lambda_1)\overline{C_1(\bar{\lambda}_3)} + 1, \\ M_{12} = A_1(\lambda_1)\overline{A_2(\bar{\lambda}_1)} + B_1(\lambda_1)\overline{B_2(\bar{\lambda}_1)} + C_1(\lambda_1)\overline{C_2(\bar{\lambda}_1)} + A_2(\lambda_1)\overline{A_2(\bar{\lambda}_2)} + B_2(\lambda_1)\overline{B_2(\bar{\lambda}_2)} \\ + C_2(\lambda_1)\overline{C_2(\bar{\lambda}_2)} + A_3(\lambda_1)\overline{A_2(\bar{\lambda}_3)} + B_3(\lambda_1)\overline{B_2(\bar{\lambda}_3)} + C_3(\lambda_1)\overline{C_2(\bar{\lambda}_3)}, \\ M_{13} = A_1(\lambda_1)\overline{A_3(\bar{\lambda}_1)} + B_1(\lambda_1)\overline{B_3(\bar{\lambda}_1)} + C_1(\lambda_1)\overline{C_3(\bar{\lambda}_1)} + A_2(\lambda_1)\overline{A_3(\bar{\lambda}_2)} + B_2(\lambda_1)\overline{B_3(\bar{\lambda}_2)} \\ + C_2(\lambda_1)\overline{C_3(\bar{\lambda}_2)} + A_3(\lambda_1)\overline{A_3(\bar{\lambda}_3)} + B_3(\lambda_1)\overline{B_3(\bar{\lambda}_3)} + C_3(\lambda_1)\overline{C_3(\bar{\lambda}_3)}, \\ M_{21} = A_1(\lambda_2)\overline{A_1(\bar{\lambda}_1)} + B_1(\lambda_2)\overline{B_1(\bar{\lambda}_1)} + C_1(\lambda_2)\overline{C_1(\bar{\lambda}_1)} + A_2(\lambda_2)\overline{A_1(\bar{\lambda}_2)} + B_2(\lambda_2)\overline{B_1(\bar{\lambda}_2)} \\ + C_2(\lambda_2)\overline{C_1(\bar{\lambda}_2)} + A_3(\lambda_2)\overline{A_1(\bar{\lambda}_3)} + B_3(\lambda_2)\overline{B_1(\bar{\lambda}_3)} + C_3(\lambda_2)\overline{C_1(\bar{\lambda}_3)}, \\ M_{22} = A_1(\lambda_2)\overline{A_2(\bar{\lambda}_1)} + B_1(\lambda_2)\overline{B_2(\bar{\lambda}_1)} + C_1(\lambda_2)\overline{C_2(\bar{\lambda}_1)} + A_2(\lambda_2)\overline{A_2(\bar{\lambda}_2)} + B_2(\lambda_2)\overline{B_2(\bar{\lambda}_2)} \\ + C_2(\lambda_2)\overline{C_2(\bar{\lambda}_2)} + A_3(\lambda_2)\overline{A_2(\bar{\lambda}_3)} + B_3(\lambda_2)\overline{B_2(\bar{\lambda}_3)} + C_3(\lambda_2)\overline{C_2(\bar{\lambda}_3)} + 1, \\ M_{23} = A_1(\lambda_2)\overline{A_3(\bar{\lambda}_1)} + B_1(\lambda_2)\overline{B_3(\bar{\lambda}_1)} + C_1(\lambda_2)\overline{C_3(\bar{\lambda}_1)} + A_2(\lambda_2)\overline{A_3(\bar{\lambda}_2)} + B_2(\lambda_2)\overline{B_3(\bar{\lambda}_2)} \\ + C_2(\lambda_2)\overline{C_3(\bar{\lambda}_2)} + A_3(\lambda_2)\overline{A_3(\bar{\lambda}_3)} + B_3(\lambda_2)\overline{B_3(\bar{\lambda}_3)} + C_3(\lambda_2)\overline{C_3(\bar{\lambda}_3)}, \\ M_{31} = A_1(\lambda_3)\overline{A_1(\bar{\lambda}_1)} + B_1(\lambda_3)\overline{B_1(\bar{\lambda}_1)} + C_1(\lambda_3)\overline{C_1(\bar{\lambda}_1)} + A_2(\lambda_3)\overline{A_1(\bar{\lambda}_2)} + B_2(\lambda_3)\overline{B_1(\bar{\lambda}_2)} \\ + C_2(\lambda_3)\overline{C_1(\bar{\lambda}_2)} + A_3(\lambda_3)\overline{A_1(\bar{\lambda}_3)} + B_3(\lambda_3)\overline{B_1(\bar{\lambda}_3)} + C_3(\lambda_3)\overline{C_1(\bar{\lambda}_3)}, \\ M_{32} = A_1(\lambda_3)\overline{A_2(\bar{\lambda}_1)} + B_1(\lambda_3)\overline{B_2(\bar{\lambda}_1)} + C_1(\lambda_3)\overline{C_2(\bar{\lambda}_1)} + A_2(\lambda_3)\overline{A_2(\bar{\lambda}_2)} + B_2(\lambda_3)\overline{B_2(\bar{\lambda}_2)} \\ + C_2(\lambda_3)\overline{C_2(\bar{\lambda}_2)} + A_3(\lambda_3)\overline{A_2(\bar{\lambda}_3)} + B_3(\lambda_3)\overline{B_2(\bar{\lambda}_3)} + C_3(\lambda_3)\overline{C_2(\bar{\lambda}_3)},$$

$$M_{33} = A_1(\lambda_3)\overline{A_3(\bar{\lambda}_1)} + B_1(\lambda_3)\overline{B_3(\bar{\lambda}_1)} + C_1(\lambda_3)\overline{C_3(\bar{\lambda}_1)} + A_2(\lambda_3)\overline{A_3(\bar{\lambda}_2)} + B_2(\lambda_3)\overline{B_3(\bar{\lambda}_2)} \\ + C_2(\lambda_3)\overline{C_3(\bar{\lambda}_2)} + A_3(\lambda_3)\overline{A_3(\bar{\lambda}_3)} + B_3(\lambda_3)\overline{B_3(\bar{\lambda}_3)} + C_3(\lambda_3)\overline{C_3(\bar{\lambda}_3)} + 1.$$

Therefore, we deduce that the 3-soliton solutions of the three-coupled fourth-order NLS systems (1.1) take the following form

$$q_1 = \overline{\left(-2i \frac{\det M^{(1)}}{\det M} \right)}, \quad q_2 = \overline{\left(-2i \frac{\det M^{(2)}}{\det M} \right)}, \quad q_3 = \overline{\left(-2i \frac{\det M^{(3)}}{\det M} \right)}. \quad (4.12)$$

Similarly, the 3-soliton solutions are derived from the general expression (4.2) by taking $N = 3$. While the exact forms of the solution components are lengthy and omitted here, the corresponding dynamics are clearly demonstrated through the plots in Figures 8–10, confirming the validity of the general formula.

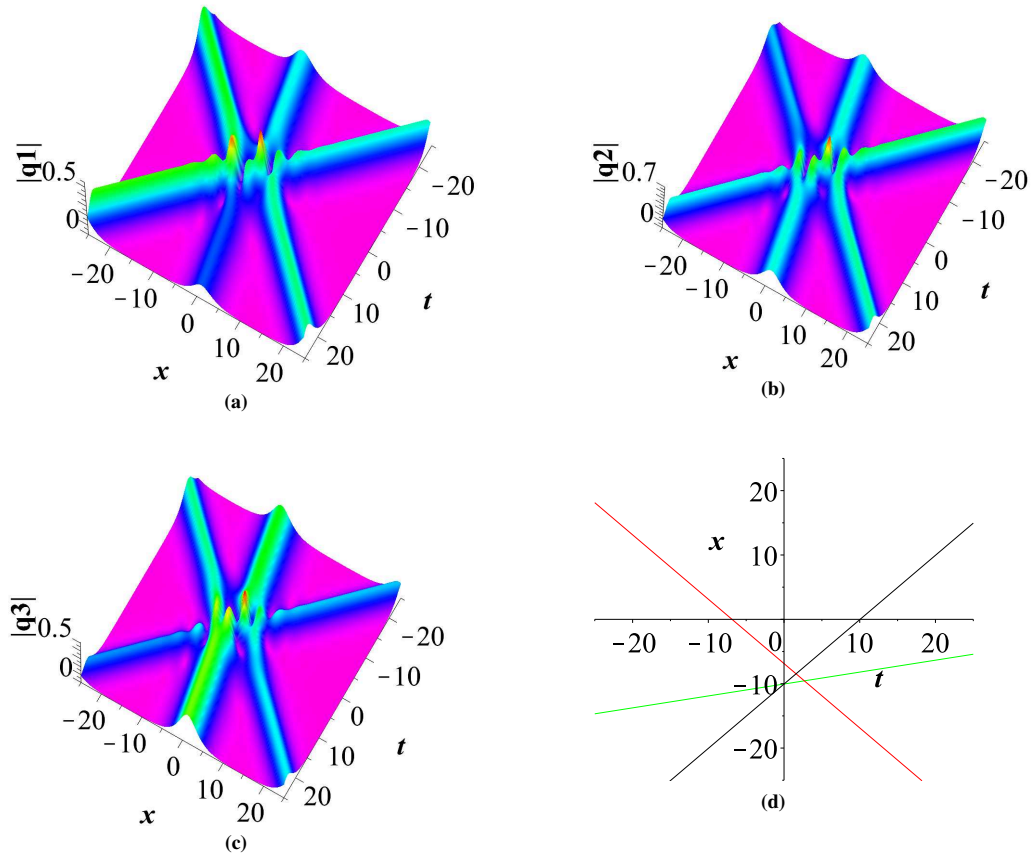


Figure 8. The 3-soliton solution (4.12) for Eq (1.1) with the parameters $\zeta_1 = -\frac{5}{12}$, $\beta_1 = \frac{1}{4}$, $\zeta_2 = \frac{1}{4}$, $\beta_2 = -\frac{1}{4}$, $\zeta_3 = -\frac{1}{4}$, $\beta_3 = \frac{1}{4}$, $c_{1,1} = \frac{1}{4}$, $c_{1,2} = \frac{1}{3}$, $c_{1,3} = \frac{1}{3}$, $c_{2,1} = \frac{1}{3}$, $c_{2,2} = \frac{1}{2}$, $c_{2,3} = \frac{1}{3}$, $c_{3,1} = \frac{1}{3}$, $c_{3,2} = \frac{1}{4}$, $c_{3,3} = \frac{1}{4}$, and $\gamma = 1$; (a) Three-dimensional plot of q_1 ; (b) Three-dimensional plot of q_2 ; (c) Three-dimensional plot of q_3 ; (d) The characteristic line $L_1 : x = \frac{5}{27}t + 8 \ln(\frac{41}{144})$, $L_2 : x = -t + 8 \ln(\frac{61}{144})$ and $L_3 : x = t + 8 \ln(\frac{41}{144})$.

In addition, following the same approach used for the 1-soliton and 2-soliton solutions, we assume

that $\lambda_1 = \zeta_1 + i\beta_1$, $\lambda_2 = \zeta_2 + i\beta_2$ and $\lambda_3 = \zeta_3 + i\beta_3$. Under these assumptions, we derive that the 3-soliton solutions possess the following two characteristic lines

$$\begin{aligned} L_1 : \beta_1 x + 4(8\zeta_1\beta_1^3\gamma - 8\zeta_1^3\beta_1\gamma + \zeta_1\beta_1)t - \frac{1}{2\beta_1} \ln(c_{1,1}\bar{c}_{1,1} + c_{2,1}\bar{c}_{2,1} + c_{3,1}\bar{c}_{3,1}) &= 0, \\ L_2 : \beta_2 x + 4(8\zeta_2\beta_2^3\gamma - 8\zeta_2^3\beta_2\gamma + \zeta_2\beta_2)t - \frac{1}{2\beta_2} \ln(c_{1,2}\bar{c}_{1,2} + c_{2,2}\bar{c}_{2,2} + c_{3,2}\bar{c}_{3,2}) &= 0, \\ L_3 : \beta_3 x + 4(8\zeta_3\beta_3^3\gamma - 8\zeta_3^3\beta_3\gamma + \zeta_3\beta_3)t - \frac{1}{2\beta_3} \ln(c_{1,3}\bar{c}_{1,3} + c_{2,3}\bar{c}_{2,3} + c_{3,3}\bar{c}_{3,3}) &= 0. \end{aligned}$$

Figures 8–10 illustrate the dynamic behavior of 3-soliton solutions of the coupled fourth-order NLS system under various parameter settings. These interactions reveal the complex and diverse nature of multi-soliton collisions, reflecting both the system's strong nonlinearity and its underlying integrable structure.

In Figure 8, the spectral parameters are chosen as $\zeta_1 = -\frac{5}{12}$, $\zeta_2 = \frac{1}{4}$, and $\zeta_3 = -\frac{1}{4}$, resulting in an asymmetric distribution in the complex plane. This asymmetry leads to non-uniform propagation paths and uneven interaction dynamics among the three solitons. The characteristic lines L_1 , L_2 , and L_3 reveal that solitons 1 and 2 undergo a direct collision followed by rapid separation, while soliton 3, due to its distinct spectral configuration, experiences a noticeable trajectory shift. Consequently, the overall three-soliton interaction manifests as a cascade of pairwise collisions. Although the system eventually restores a multi-soliton structure, slight deformation in the soliton profiles indicates weakly inelastic behavior during the interaction process.

In Figure 9, the spectral parameters are set as $\zeta_1 = -\frac{1}{6}$, $\zeta_2 = \frac{1}{4}$, and $\zeta_3 = -\frac{1}{4}$, yielding a configuration with closer spacing and partial symmetry. From the three-dimensional plots and two-dimensional density maps, it can be observed that solitons 1 and 2 propagate forward in parallel, while soliton 3 subsequently collides with them, leading to a complex three-soliton coupling effect. This sequence and timing of collisions can be interpreted as a manifestation of the collective dynamics within the soliton ensemble. In particular, the phase shifts and trajectory deviations observed during the evolution further demonstrate the nontrivial interference characteristics intrinsic to the soliton solutions in this system.

In Figure 10, the spectral parameters are set as $\zeta_1 = -\frac{5}{12}$, $\zeta_2 = \frac{1}{12}$, and $\zeta_3 = \frac{1}{3}$. The resulting interaction initially forms a tightly bound cluster, where all three soliton peaks converge in space-time, creating a pronounced interference region. The two-dimensional density plots (Figure 10 (d)–(f)) reveal localized zones of high amplitude and interference fringes during the collision phase. This can be interpreted as a transient resonant structure involving all three solitons. Following the collision, the solitons rapidly separate and regain their individual profiles and trajectories, indicating a quasi-elastic scattering process with minimal residual distortion.

The results presented in Figures 8–10 collectively highlight several key physical insights into the nature of three-soliton interactions within the coupled fourth-order NLS system. These interactions exhibit pronounced asymmetry, weakly inelastic deformation, and distinct nonlinear interference patterns, all of which are intricately shaped by the configuration and spacing of the underlying spectral parameters. The characteristic lines L_1 , L_2 , and L_3 clearly delineate the geometric structure of soliton trajectories, serving as a powerful framework for interpreting the observed scattering behavior. These findings hold potential relevance for practical applications in nonlinear optical wave guides, phase-controlled beam networks, and coupled quantum field systems, especially in scenarios involving multimode interference in Bose-Einstein condensates.

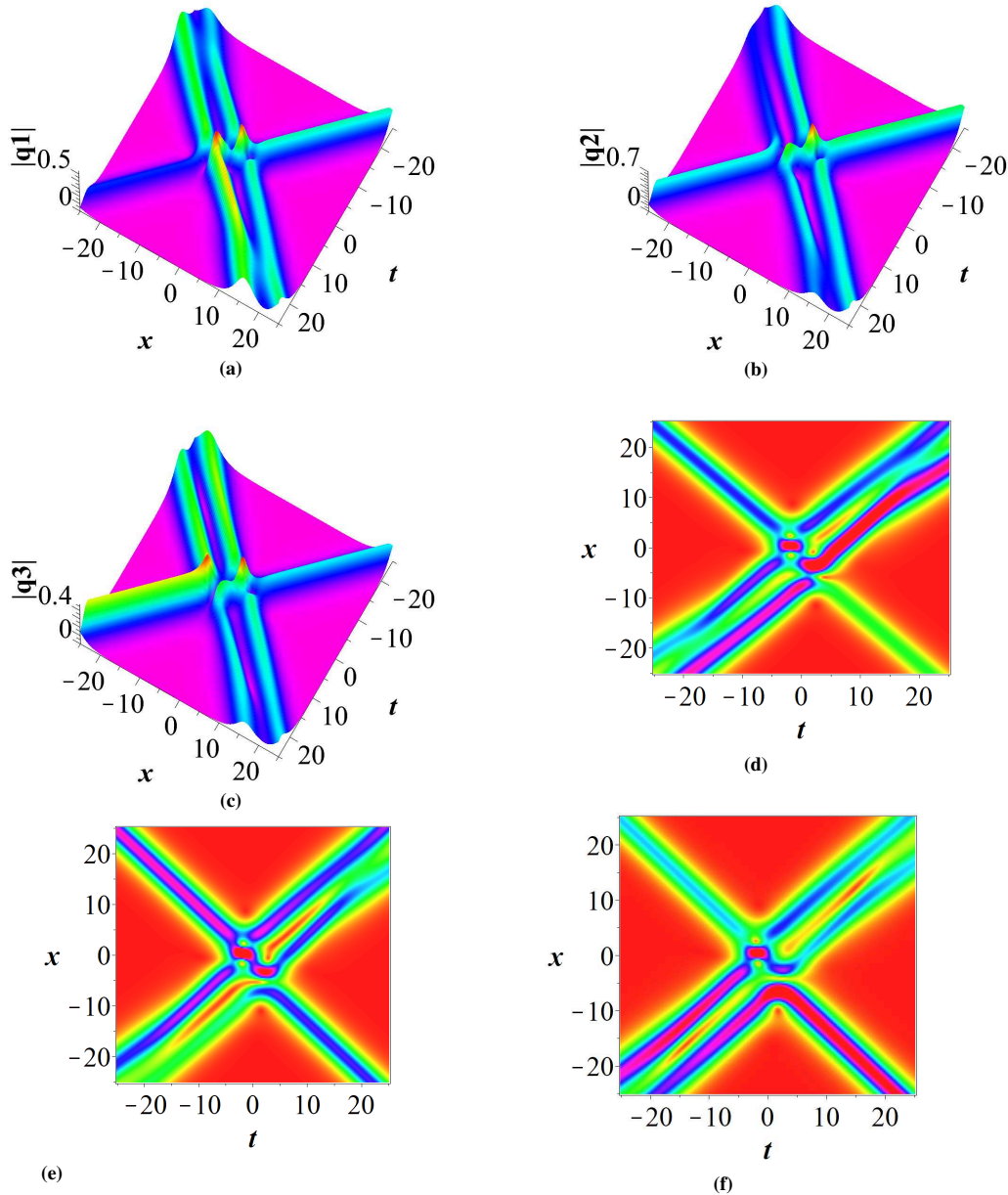


Figure 9. The 3-soliton solution (4.12) for Eq. (1.1) with the parameters $\zeta_1 = -\frac{1}{6}$, $\beta_1 = \frac{1}{4}$, $\zeta_2 = \frac{1}{4}$, $\beta_2 = -\frac{1}{4}$, $\zeta_3 = -\frac{1}{4}$, $\beta_3 = \frac{1}{4}$, $c_{1,1} = \frac{1}{4}$, $c_{1,2} = \frac{1}{3}$, $c_{1,3} = \frac{1}{3}$, $c_{2,1} = \frac{1}{3}$, $c_{2,2} = \frac{1}{2}$, $c_{2,3} = \frac{1}{3}$, $c_{3,1} = \frac{1}{3}$, $c_{3,2} = \frac{1}{4}$, $c_{3,3} = \frac{1}{4}$, and $\gamma = 1$; (a) Three-dimensional plot of q_1 ; (b) Three-dimensional plot of q_2 ; (c) Three-dimensional plot of q_3 ; (d) Two-dimensional density plot of q_1 ; (e) Two-dimensional density plot of q_2 ; (f) Two-dimensional density plot of q_3 .

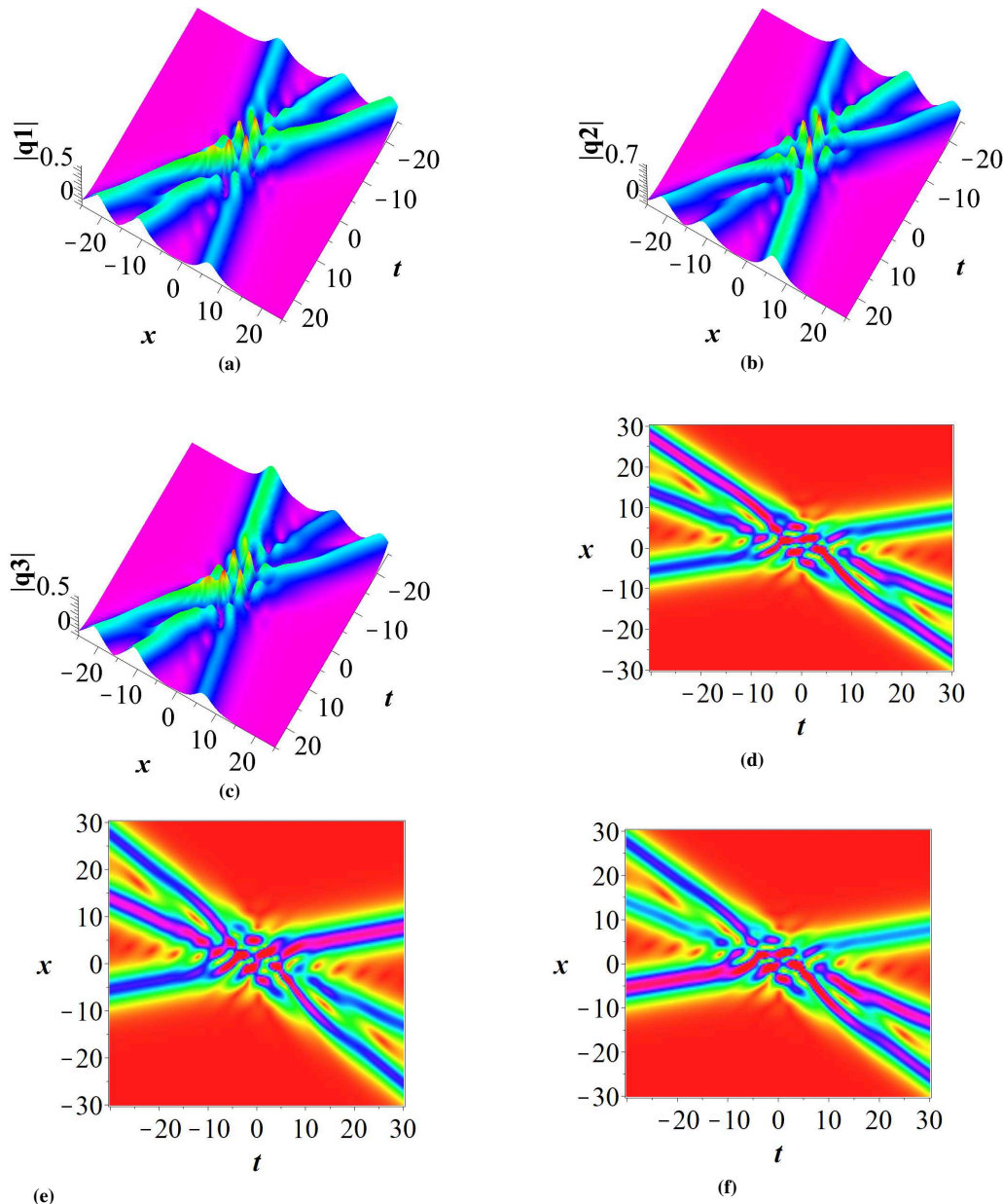


Figure 10. The 3-soliton solution (4.12) for Eq (1.1) with the parameters $\zeta_1 = -\frac{5}{12}$, $\beta_1 = \frac{1}{4}$, $\zeta_2 = \frac{1}{12}$, $\beta_2 = -\frac{1}{4}$, $\zeta_3 = \frac{1}{3}$, $\beta_3 = \frac{1}{4}$, $c_{1,1} = \frac{1}{4}$, $c_{1,2} = \frac{1}{3}$, $c_{1,3} = \frac{1}{3}$, $c_{2,1} = \frac{1}{3}$, $c_{2,2} = \frac{1}{2}$, $c_{2,3} = \frac{1}{3}$, $c_{3,1} = \frac{1}{3}$, $c_{3,2} = \frac{1}{4}$, $c_{3,3} = \frac{1}{4}$, and $\gamma = 1$; (a) Three-dimensional plot of q_1 ; (b) Three-dimensional plot of q_2 ; (c) Three-dimensional plot of q_3 ; (d) Two-dimensional density plot of q_1 ; (e) Two-dimensional density plot of q_2 ; (f) Two-dimensional density plot of q_3 .

4.3. Asymptotic analysis of soliton interactions

In the framework of the $\bar{\partial}$ -dressing method, the N -soliton solutions of the three-coupled fourth-order NLS systems are constructed by choosing N discrete spectral points $\lambda_j = \zeta_j + i\beta_j$ ($j = 1, \dots, N$)

in the complex plane, together with associated constant vectors $\mathbf{c}_{h,j}$ (the so-called norming data). The analytic properties of the resulting integral equation allow one to extract physical quantities of each soliton.

Velocity. In the $\bar{\partial}$ -formulation, the phase of each exponential term in the reconstructed solution involves a term of the form

$$\theta_j(x, t) = -\lambda_j x + \Omega(\lambda_j)t,$$

where $\Omega(\lambda)$ is the dispersion relation derived from the associated Lax pair. For the three-coupled fourth-order NLS systems, we have

$$\Omega(\lambda) = 8\gamma\lambda^4 - 2\lambda^2.$$

Hence, the trajectory of constant phase satisfies

$$-x + (8\gamma\lambda_j^3 - 2\lambda_j)t = \text{const},$$

which implies that the velocity of the j -th soliton is given by

$$v_j = 4(8\gamma\zeta_j^3 - 8\gamma\zeta_j\beta_j^2 - \zeta_j). \quad (4.13)$$

Amplitude. The amplitude of each soliton is linked to the imaginary part β_j of its corresponding spectral parameter, as well as the residue of the pole in the integral representation. More precisely, under standard normalization, the peak amplitude A_j is proportional to β_j

$$A_j \propto \beta_j,$$

reflecting the exponential localization in the spatial direction.

Phase Shift. The $\bar{\partial}$ -dressing method yields nonlinear superposition effects when multiple solitons are constructed using several discrete spectral points. The interaction-induced phase shift can be computed from the logarithmic terms appearing in the determinant structure of the solution. In the 2-soliton case, the phase shift $\Delta\phi_j$ of the j -th soliton due to interaction with another soliton at λ_k is given by

$$\Delta\phi_j = \ln \left| \frac{(\lambda_j - \bar{\lambda}_k)(\bar{\lambda}_j - \lambda_k)}{(\lambda_j - \lambda_k)(\bar{\lambda}_j - \bar{\lambda}_k)} \right|. \quad (4.14)$$

This expression shows that the shift depends on the spectral parameter difference and hence on both the velocity and amplitude of the interacting solitons.

This analysis not only confirms the elastic nature of the soliton interactions in this system but also highlights the nontrivial coupling effects among the three components. Representative plots and simulations are provided in Figures 1-10. to support the theoretical findings. In conclusion, the $\bar{\partial}$ -dressing method not only provides a powerful tool for constructing explicit multi-soliton solutions, but also offers a clear analytic path to study the internal structure and dynamics of soliton interactions in the three-component fourth-order NLS system.

5. Conclusions and discussions

In this work, we have constructed and analyzed new explicit solutions for the three-coupled fourth-order NLS systems (1.1) by employing the $\bar{\partial}$ -dressing method. A 4×4 matrix $\bar{\partial}$ -equation was introduced to derive the corresponding spatial and temporal spectral problems, from which a special $\bar{\partial}$ -problem was formulated and solved using the Cauchy CGreen integral operator. This approach enabled us to obtain the N -soliton solutions of the three-coupled fourth-order NLS systems, demonstrating the efficiency and flexibility of the $\bar{\partial}$ -dressing method in generating soliton solutions for complex nonlinear evolution equations.

Moreover, by introducing recursive operators, we established the three-coupled fourth-order NLS hierarchy and derived explicit expressions for the 1-, 2-, and 3-soliton solutions. Their corresponding three-dimensional visualizations clearly reveal the rich interaction dynamics among multiple soliton components, providing deeper insight into nonlinear wave propagation in coupled systems.

The present study thus establishes a universal and systematic framework for analyzing higher-order, multi-component integrable systems through the $\bar{\partial}$ -dressing method. This framework can be readily extended to other nonlinear models with similar algebraic structures, serving as a powerful analytical tool for exploring a broad class of physical systems. In future work, this methodology may be further extended to systems with non-vanishing boundary conditions or applied to other multi-component physical models such as coupled nonlinear Schrödinger equations, spinor Bose Einstein condensates, and optical fiber systems. Such investigations would not only deepen our understanding of nonlinear phenomena in multi-component and higher-order contexts but may also uncover new aspects of integrable dynamics.

Use of Generative-AI tools declaration

The author(s) declare(s) they have used Artificial Intelligence (AI) tools in the creation of this article.

AI tools used: DeepSeek (by DeepSeek Company).

How were the AI tools used? The DeepSeek AI assistant was employed exclusively for text polishing and language enhancement. Specifically, it was used to: Revise sentences for improved clarity, fluency, and academic tone. Correct minor grammatical errors and refine word choice. Ensure consistency in technical terminology. The core research ideas, mathematical derivations, computational results, data analysis, conclusions, and the substantive intellectual content of the work are entirely the author(s)' own. The use of AI was strictly limited to auxiliary language editing and did not involve generating original scientific ideas, interpretations, or data.

Where in the article is the information located? The AI-assisted language polishing was applied throughout the manuscript to improve readability. This includes the Introduction, Methodology, and Discussion sections. All edits were thoroughly reviewed, validated, and approved by the authors.

Author contributions

Xue-Wei Yan: Software, Supervision, Validation. Jin-Jin Mao: Conceptualization, Data curation, Formal analysis, Funding acquisition, Investigation, Methodology, Project administration, Resources,

Visualization, Writing-original draft, Writing-review & editing.

Acknowledgements

Natural Science Research Start-up Foundation of Recruiting Talents of Nanjing University of Posts and Telecommunications (Grant No. NY225004).

Conflict of interest

The authors declare that they have no competing interests.

References

1. G. P. Agrawal, Nonlinear Fiber Optics, Berlin, Heidelberg: Springer Berlin Heidelberg, **542** (2000), 195–211. https://doi.org/10.1007/3-540-46629-0_9
2. D. R. Solli, C. Ropers, P. Koonath, B. Jalali, Optical rogue waves, *Nature*, **450** (2007), 1054–1057. <https://doi.org/10.1038/nature06402>
3. D. R. Solli, C. Ropers, B. Jalali, Active control of rogue waves for stimulated supercontinuum generation, *Phys. Rev. Lett.*, **101** (2008), 233902. <https://doi.org/10.1103/PhysRevLett.101.233902>
4. W. M. Moslem, P. Shukal, B. Eliasson, *EPL*, **96** (2011), 25002.
5. Z. Du, B. Tian, Q. X. Qu, H. P. Chai, X. Y. Wu, Semirational rogue waves for the three-coupled fourth-order nonlinear Schrödinger equations in an alpha helical protein, *Superlattice. Microst.*, **112** (2017), 362–373. <https://doi.org/10.1016/j.spmi.2017.09.046>
6. A. Chabchoub, N. Hoffmann, H. Branger, C. Kharuf, N. Akhmediev, Experiments on wind-perturbed rogue wave hydrodynamics using the Peregrine breather model, *Phys. Fluids.*, **25** (2013), 101704. <https://doi.org/10.1063/1.4824706>
7. Z. Y. Yan, Financial rogue waves, *Commun. Theor. Phys.*, **54** (2010), 947–949. <https://doi.org/10.1088/0253-6102/54/5/31>
8. L. Stenflo, P. Shukla, J. Plasma, Nonlinear acoustic-gravity waves, *J. Plasma Phys.*, **75** (2009), 841–847. <https://doi.org/10.1017/S0022377809007892>
9. L. Ling, L. C. Zhao, B. Guo, Darboux transformation and multi-dark soliton for N-component nonlinear Schrödinger equations, *Nonlinearity*, **28** (2015), 3243–3261. <https://doi.org/10.1088/0951-7715/28/9/3243>
10. G. Zhang, Z. Yan, Three-component nonlinear Schrödinger equations: modulational instability, Nth-order vector rational and semi-rational rogue waves, and dynamics, *Commun. Nonlinear Sci.*, **62** (2018), 117–133. <https://doi.org/10.1016/j.cnsns.2018.02.008>
11. G. Mu, Z. Qin, R. Grimshaw, N. Akhmediev, Intricate dynamics of rogue waves governed by the Sasa-Satsuma equation, *Physica D*, **402** (2020), 132252. <https://doi.org/10.1016/j.physd.2019.132252>

12. C. R. Zhang, B. Tian, Q. X. Qu, L. Liu, H. Y. Tian, Vector bright solitons and their interactions of the couple Fokas-Lenells system in a birefringent optical fiber, *Z. Angew. Math. Phys.*, **71** (2020), 1–19. <https://doi.org/10.1007/s00033-019-1225-9>

13. R. Hirota, J. Satsuma, Soliton solutions of a coupled Korteweg-de Vries equation, *Phys. Lett. A.*, **85** (1981), 407–408. [https://doi.org/10.1016/0375-9601\(81\)90423-0](https://doi.org/10.1016/0375-9601(81)90423-0)

14. L. Liu, B. Tian, W. R. Sun, H. L. Zhen, W. R. Shen, Bright-dark vector soliton solutions for a generalized coupled Hirota system in the optical glass fiber, *Commun. Nonlinear. Sci.*, **39** (2016), 545–555. <https://doi.org/10.1016/j.cnsns.2016.04.001>

15. A. C. Newell, Solitons in Mathematics and Physics, Society for Industrial and applied Mathematics, 1985. <https://pubs.siam.org/doi/pdf/10.1137/1.9781611970227.fm>

16. M. J. Ablowitz, H. Segur, Solitons and the Inverse Scattering Transform, Society for Industrial and applied Mathematics, 1981. <https://pubs.siam.org/doi/pdf/10.1137/1.9781611970883.bm>

17. S. Novikov, S. V. Manakov, L. P. Pitaevskii, V. E. Zakharov, Theory of solitons: The inverse scattering method, Springer Science Business Media, 1984.

18. M. J. Ablowitz, Z. H. Musslimani, Inverse scattering transform for the integrable nonlocal nonlinear Schrödinger equation, *Nonlinearity*, **29** (2016), 915–946. <https://doi.org/10.1088/0951-7715/29/3/915>

19. D. Wang, Z. Liu, H. Zhao, H. Qin, G. Bai. C. Chen, et al., Launching by cavitation, *Science*, **389** (2025), 935–939. <https://doi.org/10.1126/science.adu8943>

20. D. S. Mou, Z. Z. Si, W. X. Qiu, C. Q. Dai, Optical soliton formation and dynamic characteristics in photonic Moiré lattices, *Opt. Laser Technol.*, **181** (2025), 111774. <https://doi.org/10.1016/j.optlastec.2024.111774>

21. Z. Z. Si, D. L. Wang, B. W. Zhu, Z. T. Ju, X. P. Wang, W. Liu, et al., Deep learning for dynamic modeling and coded information storage of vector-soliton pulsations in mode-locked fiber lasers, *Laser Photonics Rev.*, **18** (2024), 2400097. <https://doi.org/10.1002/lpor.202400097>

22. Z. Z. Si, Y. Y. Wang, C. Q. Dai. Switching, explosion, and chaos of multi-wavelength soliton states in ultrafast fiber lasers, *Sci. China Phys. Mech.*, **67** (2024), 274211. <https://doi.org/10.1007/s11433-023-2365-7>

23. A. C. Scott, Launching a Davydov soliton: I. Soliton analysis, *Physica Scripta*, **29** (1984), 279. <https://doi.org/10.1088/0031-8949/29/3/016>

24. S. S. Veni, M. M. Latha, A generalized Davydov model with interspine coupling and its integrable discretization, *Phys. Scripta*, **86** (2012), 25003. <https://doi.org/10.1088/0031-8949/86/02/025003>

25. W. R. Sun, B. Tian, Y. F. Wang, H. L. Zhen, Soliton excitations and interactions for the three-coupled fourth-order nonlinear Schrödinger equations in the alpha helical proteins, *Eur. Phys. J. D*, **69** (2015), 1–9. <https://doi.org/10.1140/epjd/e2015-60027-6>

26. Z. Du, B. Tian, H. P. Chai, Y. Q. Yuan, Vector multi-rogue waves for the three-coupled fourth-order nonlinear Schrödinger equations in an alpha helical protein, *Commun. Nonlinear. Sci.*, **67** (2019), 49–59. <https://doi.org/10.1016/j.cnsns.2018.06.014>

27. Z. Du, B. Tian, H. P. Chai, X. H. Zhao, Lax pair, Darboux transformation and rogue waves for the three-coupled fourth-order nonlinear Schrödinger system in an alpha helical protein, *Wave. Random Complex*, **31** (2021), 1051–1071. <https://doi.org/10.1080/17455030.2019.1644466>

28. M. J. Dong, L. X. Tian, J. D. Wei, Infinitely many conservation laws and Darboux-dressing transformation for the three-coupled fourth-order nonlinear Schrödinger equations, *Eur. Phys. J. Plus.*, **137** (2022), 1–15. <https://doi.org/10.1140/epjp/s13360-021-02200-6>

29. L. C. Zhao, J. Liu, Rogue-wave solutions of a three-component coupled nonlinear Schrödinger equation, *Phys. Rev. E.*, **87** (2013), 013201. <https://doi.org/10.1103/PhysRevE.87.013201>

30. X. B. Wang, B. Han, The three-component coupled nonlinear Schrödinger equation: Rogue waves on a multi-soliton background and dynamics, *EPL*, **126** (2019), 15001. <https://doi.org/10.1209/0295-5075/126/15001>

31. F. Baronio, A. Degasperis, M. Conforti, S. Wabnitz, Solutions of the vector nonlinear Schrödinger equations: Evidence for deterministic rogue waves, *Phys. Rev. Lett.*, **109** (2012), 044102. <https://doi.org/10.1103/PhysRevLett.109.044102>

32. V. E. Zakharov, A. B. Shabat, A scheme for integrating the nonlinear equations of mathematical physics by the method of the inverse scattering problem, *I. Funct. Anal. Appl.*, **8** (1974), 43–53. <https://doi.org/10.1007/BF01075696>

33. Q. Y. Cheng, Y. L. Yang, E. G. Fan, Long-time asymptotic behavior of a mixed Schrödinger equation with weighted Sobolev initial data, *J. Math. Phys.*, **62** (2021), 093507. <https://doi.org/10.1063/5.0045970>

34. Y. L. Yang, E. G. Fan, On asymptotic approximation of the modified Camassa-Holm equation in different space-time solitonic regions, 2021. arXiv preprint arXiv:2101.02489. <https://doi.org/10.48550/arXiv.2101.02489>

35. R. Beals, R. R. Coifman, The D-bar approach to inverse scattering and nonlinear evolutions, *Physica D*, **18** (1986), 242–249. [https://doi.org/10.1016/0167-2789\(86\)90184-3](https://doi.org/10.1016/0167-2789(86)90184-3)

36. R. Beals, R. R. Coifman, Linear spectral problems, non-linear equations and the $\bar{\partial}$ -method, *Inverse Probl.*, **5** (1989), 87–130. <https://doi.org/10.1088/0266-5611/5/2/002>

37. A. S. Fokas, V. E. Zakharov, The dressing method and nonlocal Riemann-Hilbert problem, *J. Nonlinear Sci.*, **2** (1992), 109–134. <https://doi.org/10.1007/BF02429853>

38. J. Zhu, X. Geng, The AB equations and the $\bar{\partial}$ -dressing method in semi-characteristic coordinates, *Math. Phys. Anal. Geom.*, **17** (2014), 49–65. <https://doi.org/10.1007/s11040-014-9140-y>

39. V. G. Dubrovsky, The $\bar{\partial}$ -dressing method and the solutions with constant asymptotic values at infinity of DS-II equation, *J. Math. Phys.*, **38** (1997), 6382–6400. <https://doi.org/10.1063/1.532218>

40. J. Zhu, S. Zhou, Z. Qiao, Forced (2+1)-dimensional discrete three-wave equation, *Commun. Theor. Phys.*, **72** (2020), 015004. <https://doi.org/10.1088/1572-9494/ab5fb4>

41. P. V. Nabeleka, V. E. Zakharov, Solutions to the Kaup-Broer system and its (2 + 1) dimensional integrable generalization via the dressing method, *Physica D*, **409** (2020), 132478. <https://doi.org/10.1016/j.physd.2020.132478>

42. J. Luo, E. Fan, $\bar{\partial}$ -dressing method for the coupled Gerdjikov-Ivanov equation, *Appl. Math. Lett.*, **110** (2020), 106589. <https://doi.org/10.1016/j.aml.2020.106589>

- 43. Z. Q. Li, S. F. Tian, A hierarchy of nonlocal nonlinear evolution equations and $\bar{\partial}$ -dressing method, *Appl. Math. Lett.*, **120** (2021), 107254. <https://doi.org/10.1016/j.aml.2021.107254>
- 44. X. Wang, J. Zhu, Z. Qiao, New solutions to the differential-difference KP equation, *Appl. Math. Lett.*, **113** (2021), 106836. <https://doi.org/10.1016/j.aml.2020.106836>
- 45. M. J. Ablowitz, D. B. Yaacov, A. S. Fokas, On the inverse scattering transform for the Kadomtesev-Petviashvili equation, *Stud. Appl. Math.*, **69** (1983), 135–143. <https://doi.org/10.1002/sapm1983692135>



AIMS Press

© 2025 the Author(s), licensee AIMS Press. This is an open access article distributed under the terms of the Creative Commons Attribution License (<https://creativecommons.org/licenses/by/4.0/>)